HHS Public Access

Author manuscript

*J Immunol*. Author manuscript; available in PMC 2024 December 15.

Published in final edited form as:

*J Immunol*. 2023 December 15; 211(12): 1823–1834. doi:10.4049/jimmunol.2300351.

# HOIL1 regulates group 3 innate lymphoid cells in the colon and protects against systemic dissemination, colonic ulceration, and lethality from *Citrobacter rodentium* infection

**Victoria L. Hartley**[*], **Arwa M. Qaqish**[*,§], **Matthew J. Wood**[*,¶], **Brian T. Studnicka**[*,□], **Kazuhiro Iwai**[†], **Ta-Chiang Liu**[‡], **Donna A. MacDuff**[*,#]

[*]Department of Microbiology and Immunology, University of Illinois Chicago College of Medicine, Chicago, Illinois, USA.

[†]Department of Molecular and Cellular Physiology, Graduate School of Medicine, Kyoto University, Kyoto, Japan.

[‡]Department of Pathology and Immunology, Washington University School of Medicine, Saint Louis, Missouri, USA.

## Abstract

HOIL1-deficient patients experience chronic intestinal inflammation and diarrhea as well as increased susceptibility to bacterial infections. HOIL1 is a component of the linear ubiquitin chain assembly complex that regulates immune signaling pathways, including NF-κB-activating pathways. We have shown previously that HOIL1 is essential for survival following *Citrobacter rodentium* gastrointestinal infection of mice, but the mechanism of protection by HOIL1 was not examined. *C. rodentium* is an important murine model for human attaching and effacing (A/E) pathogens, enteropathogenic and enterohemorrhagic *Escherichia coli*, that cause diarrhea and food-borne illnesses, and lead to severe disease in children and immunocompromised individuals. In this study, we found that *C. rodentium* infection resulted in severe colitis and dissemination of *C. rodentium* to systemic organs in HOIL1-deficient mice. HOIL1 was important in the innate immune response in to limit early replication and dissemination of *C. rodentium*. Using bone marrow chimeras and cell type-specific knock-out mice, we found that HOIL1 functioned in radiation-resistant cells and partly in radiation-sensitive cells and in myeloid cells to limit disease, but was dispensable in intestinal epithelial cells. HOIL1-deficiency significantly impaired the expansion of ILC3 and their production of IL-22 during *C. rodentium* infection. Understanding the role HOIL1 plays in type 3 inflammation and in limiting the pathogenesis of A/E lesion-forming bacteria will provide further insight into the innate immune response to gastrointestinal pathogens and inflammatory disorders.

[#]Address correspondence to Donna A. MacDuff, dmacduff@uic.edu.
[§]Present address: Department of Biology and Biotechnology, Faculty of Science, The Hashemite University, Zarqa, Jordan, and Department of Cellular Therapy and Applied Genomics, King Hussein Cancer Center (KHCC), Amman, Jordan.
[¶]Present address: Department of Internal Medicine, Rush University Medical Center, Chicago, Illinois, USA.
□Present address: AbbVie, Lake Forest, Illinois, USA.

## Introduction

Enterohemorrhagic *Escherichia coli* (EHEC) and enteropathogenic *E. coli* (EPEC) infections are a leading cause of bacterial diarrheal disease and lethality in children in the developing world (1, 2). In developed countries, EPEC and EHEC are common causative agents of foodborne illnesses (3). While disease symptoms are typically mild in immunocompetent adults, infection can lead to severe morbidity and mortality in infants and immunocompromised individuals (3–5). Since EPEC and EHEC do not easily infect mice, their murine counterpart, *Citrobacter rodentium*, has been used extensively to model and investigate these pathogens *in vivo* (6, 7). EPEC, EHEC, and *C. rodentium* infections are characterized by the formation of attaching and effacing (A/E) lesions on intestinal epithelial cells (8), wherein bacteria attach directly to intestinal epithelium, efface the microvilli, and form pedestal-like structures on the epithelial cells beneath the adherent bacteria. This process is mediated by a bacterial type III secretion system that injects effector proteins into the intestinal epithelial cells, altering their metabolism, actin polymerization (9) and immune functions (7, 10, 11). *C. rodentium*-induced colitis is also used as an experimental animal model for inflammatory bowel diseases such as Crohn's disease and ulcerative colitis (12).

Following peroral inoculation of C57BL/6 mice, *C. rodentium* initially colonizes the cecum followed by the colon within two to three days (13). *C. rodentium* infection induces colitis and colonic hyperplasia, characterized by infiltration of immune cells, excessive proliferation of intestinal epithelial cells (IEC) and deepening of colonic crypts. Bacterial burdens are mostly contained within the GI tract, peaking around six to ten days post-infection, and are cleared within three weeks (13). Upon infection, pattern recognition receptors such as Toll-like receptors (TLRs) on IECs, dendritic cells (DCs) and macrophages in the intestine detect the presence of pathogenic bacteria and initiate innate immune responses. Production of cytokines such as IL-23 and IL-1β by DCs and macrophages leads to the production of IL-22 by group 3 innate lymphoid cells (ILC3) and T helper type 22 (Th22) cells (14–19). IL-22 is crucial for the early mucosal immune response to control *C. rodentium*, as it promotes barrier defense through IEC proliferation and the production of antimicrobial peptides (17, 20–22). The adaptive immune response, particularly the production of antibodies against *C. rodentium*, is essential for clearance of the pathogen and survival following infection (23).

We have shown previously that heme-oxidized IRP2 ubiquitin ligase-1 (HOIL1, official gene name *Rbck1*), a component of the Linear Ubiquitin Chain Assembly Complex (LUBAC), is essential for survival during *C. rodentium* infection (24). However, the mechanism by which HOIL1 protects against *C. rodentium*-induced pathogenesis is unknown. LUBAC is a trimeric complex composed of HOIL1, HOIP and SHARPIN. The catalytic subunit, HOIP, is the only E3 ubiquitin ligase known to generate linear (methionine-1 linked) ubiquitin chains (25–27). LUBAC has been implicated in the regulation of type 1 inflammatory cytokines downstream of multiple innate immune receptors that lead to the activation of canonical NF-κB, such as TNFR1, IL-1- and IL-17-family receptors, TLRs, and CD40, as well as in the modulation of extrinsic programmed cell death pathways (24, 26–36). HOIL1 also contains a functional E3 ubiquitin ligase domain (37, 38). However, the range of substrates ubiquitinated by HOIL1 and their downstream functions are not well understood

(37–39). In humans, HOIL1 deficiency is associated with a lethal disorder characterized by increased susceptibility to pyogenic bacterial infection, chronic autoinflammation, muscular amylopectinosis and IBD-like symptoms (40–42). Since full deletion of *Hoil1* leads to embryonic lethality in mice (43, 44), our lab uses a mouse strain that express a truncated version of HOIL1 lacking the C-terminal RING-between-RING domain to study the physiological functions of HOIL1 *in vivo* (24, 26, 43). Expression of HOIP and SHARPIN is also reduced in these mice. While these "HOIL1-mutant" mice (*Hoil1*$^{-/-}$ herein) display no overt phenotype when housed in specific pathogen-free (SPF) conditions, they are highly susceptible to certain infections including *Listeria monocytogenes, Toxoplasma gondii*, and *C. rodentium*. Additionally, *Hoil1*$^{-/-}$ mice exhibit hyperinflammation during chronic infection with *Mycobacterium tuberculosis* or murine gamma-herpesvirus 68, as well as progressive amylopectinosis in their cardiac tissue, suggesting that they are a suitable model for HOIL1-deficiency in humans (24, 40, 41). While susceptibility of *Hoil1*$^{-/-}$ mice to *Listeria* infection is associated with defective induction of type 1 inflammatory cytokines, including IL-12, TNF-α, IL-6 and interferon-gamma (IFN-γ) the role of HOIL1 in the type 3 inflammatory response to extracellular bacterial pathogens such as to *C. rodentium* has not been elucidated.

Here, we show that HOIL1 plays an essential role in the innate immune response to limit early *C. rodentium* replication in the GI tract, as well as to prevent dissemination to systemic tissues and severe colonic ulceration. HOIL1 modulated the inflammatory cytokine response, including IL-22 and CCL20, during *C. rodentium* infection. Using cell type-specific knock-out mice, we show that HOIL1 plays important roles in CD11c-expressing and lysozyme-2-expressing myeloid cells, but not in Villin 1-expressing IECs, to limit systemic dissemination and weight loss. However, HOIL1 was not required to regulate populations of these cells before or during infection. Instead, we found that HOIL1 regulates ILC populations in the colon, resulting in a decrease in the number of RORγt$^{+}$ ILC3s and IL-22-expressing ILC3s during infection. These findings highlight a key role for HOIL1 in modulating innate mucosal immunity to an A/E gastrointestinal pathogen.

## Materials and Methods

### Mice.

*Hoil1*$^{-/-}$ (B6.Cg-Hoil1$^{tm1Kiwa}$), *Rag1*$^{-/-}$*Hoil1*$^{-/-}$ and *Hoil1*$^{-/-}$*Il4ra*$^{\Delta IEC}$ mice have been described previously (24, 26, 45). Wild type control mice were either *Hoil1*$^{+/+}$ littermates or C56BL/6 mice from our colony. All phenotypes were confirmed with *Hoil1*$^{+/+}$ littermates. *Rag1*$^{-/-}$*Hoil1*$^{+/+}$ littermates were used as controls for *Rag1*$^{-/-}$*Hoil1*$^{-/-}$ mice. B6NCrl;B6N-A$^{tm1Brd}$Rbck1$^{tm1a(EUCOMM)Hmgu}$ mice were acquired from INFRAFRONTIER /EMMA (European mutant mouse archive) (46, 47). Mice were crossed to FLP deleter mice to remove the targeting cassette to generate *Rbck1*$^{+/f}$ mice, then backcrossed to B6J using speed congenics. *Rbck1*$^{+/f}$ mice were crossed to B6.C-Tg(CMV-cre)1Cgn/J mice (Cre deleter, Jackson labs) to delete the floxed region. *Rbck1*$^{+/-}$ mice were crossed to *Rbck1*$^{f/f}$ and generate *Rbck1*$^{f/-}$ mice. Mice were crossed to B6.Cg-Tg(Vil1-cre)1000Gum/J to generate *Rbck1*$^{f/-\ Vil1\text{-}cre}$ mice, to B6.Cg-Tg(Itgax-cre)1–1Reiz/J mice to generate *Rbck1*$^{f/-\ CD11c\text{-}cre}$ mice, or to B6.129P2-Lyz2tm1(cre)Ifo/J to generate *Rbck1*$^{f/-\ Lyz2\text{-}cre}$

mice. Mice were age-matched for individual experiments. Mice were cohoused and littermate controls were used. Both male and female mice were used, as sex differences were not observed. Mice were housed and bred at Washington University in Saint Louis or at University of Illinois Chicago in specific pathogen-free conditions in accordance with Federal and University guidelines, and protocols were approved by the Animal Studies Committee of Washington University or the Animal Care Committee of the University of Illinois Chicago.

### *In vivo* infections.

Kanamycin-resistant *C. rodentium* strain DBS120 was used for this study (48). Bacteria were grown in Luria-Bertani (LB) medium containing 50 μg/ml kanamycin at 37°C. Mice between six and eight wks-of-age were inoculated intragastrically (i.g.) with $2\times10^9$ CFU from a log-phase culture in 100 μl 3% sodium bicarbonate in PBS. For i.p. infections, mice were injected with $2\times10^7$ CFU *C. rodentium* in 300 μl PBS into the peritoneal cavity. Mice were monitored daily for morbidity and mortality, and mice that had lost more than 30% of their initial body weight were euthanized.

Stool samples were collected every two days and analyzed for colony forming units (CFU). Mice that were not shedding detectable amounts of *C. rodentium* by 4 dpi were excluded from the study. Upon euthanasia, organ pieces were placed in pre-weighed sterile tubes containing 1.0 mm zirconia/silica beads (BioSpec Products Inc.) on ice for analysis of CFU, or snap-frozen and stored at −80°C for future RNA or protein analysis. To determine CFU, fresh organ and stool samples were homogenized in 1 ml PBS plus 0.1% Tween 20 with a mini-beadbeater (BioSpec Products Inc.), serially diluted in PBS plus 0.1% Tween 20, and plated on LB agar containing 50 μg/ml kanamycin.

### Generation of bone marrow chimeric mice.

Bone marrow transplants were performed as described previously (24). Briefly, recipient mice were exposed to 1200 rad of whole body irradiation, and injected i.v. with 10 million whole bone marrow cells from donor mice. Mice were allowed to reconstitute for 16 wks before inoculation with *C. rodentium*. Mice were bled at 14 wks post-irradiation to determine percent chimerism by quantitative PCR (qPCR) on genomic DNA isolated from peripheral blood as described previously (24).

### Infection of bone marrow-derived macrophages and dendritic cells.

Primary bone marrow-derived macrophages (BMDMs) and bone marrow-derived DCs (BMDCs) were prepared as described previously (49, 50). For cytokine mRNA and protein analyses, BMDMs were differentiated for 7 d, then scraped, seeded in tissue culture-treated plates, and allowed to adhere for 3 d. BMDCs were differentiated for 7 d, suspension cells collected, and plated immediately prior to infection. Cells were infected with log-phase *C. rodentium* at an MOI of 5. At 2 hpi, media were aspirated and fresh media containing 50 U/ml penicillin, 50 μg/ml streptomycin, and 100 μg/ml gentamicin were added to kill *C. rodentium*. Cells were lysed in Tri-Reagent (Sigma) for RNA extraction. Cell supernatants were collected and stored at −80°C for cytokine analysis.

### qRT-PCR.

Frozen tissue samples were homogenized in 1 ml TRI Reagent (Sigma) and RNA was isolated according to the manufacturer's instructions. RNA samples were treated with Turbo DNA-free DNase (Ambion). cDNA synthesis was performed using Improm-II (Promega) and random hexamer primers. qPCR was performed using a StepOnePlus or QuantStudio 3 real-time PCR system (Applied Biosystems) with Amplitaq Gold polymerase (Applied Biosystems) and PrimeTime probe-based qPCR Assays (Integrated DNA Technologies) specific for *Cxcl1* (Mm.PT.58.42076891), *Il23a* (Mm.PT.58.10594618.g), *Il6* (Mm.PT.58.10005566), *Tnf* (Mm.PT.58.12575861), *Il1b* (Mm.PT.58.41616450), *Il12b* (Mm.PT.58.12409997), *Ifng* (Mm.Pt.58.41769240), *Il13* (Mm.PT.58.31366752) and *Il22* (F: AGA ACG TCT TCC AGG GTG AA; R: TCC GAG GAG TCA GTG CTA A; Probe: /56-FAM/TGA GCA CCT GCT TCA TCA GGT AGC A/36-TAMSp/). Transcripts were quantitated using specific standard curves and copy numbers normalized to the reference gene *Rps29* (forward primer 5′-GCA AAT ACG GGC TGA ACA TG-3′, reverse primer 5′-GTC CAA CTT AAT GAA GCC TAT GTC-3′, and probe 5'-/5HEX/CCT TCG CGT/ZEN/ ACT GCC GGA AGC/ 3IABkFQ/−3' (Integrated DNA Technologies).

### Histological analyses.

Intestinal tissue was flushed with PBS and fixed in 10% neutral-buffered formalin at 4°C for 20 h, washed three times with 70% ethanol and incubated in 70% ethanol at 4°C for at least 24 h. Colons and cecums were cut into strips, embedded in 2% agar for optimal crypt orientation prior to being embedded in paraffin, sectioned, and stained with H&E. Imaging was performed on a BZ-X710 microscope (Keyence). Histologic severity scores were assigned based on a pre-determined, semi-quantitative histologic severity score (51). Briefly, 0: no neutrophils; 1: neutrophils in surface epithelium, lamina propria, or cryptitis; 2: crypt abscess; 3: neutrophilic inflammation present at muscularis mucosae or submucosa; 4: ulcer or transmural inflammation; 5: epithelial denudement. The percentage of longitudinal involved colon was also quantified.

### Intestinal permeability analyses.

150 μl of 80 mg/ml fluorescein isothiocyanate dextran (FITC-dextran, FD4, Sigma) in PBS was administered to mice by oral gavage. 4 h after administration, mice were euthanized with $CO_2$, and blood was collected by cardiac puncture, transferred to a Microtainer Serum Separator tube (BD), and processed according to the manufacturer's instructions. FITC-dextran concentration in the serum was determined by spectrophotofluorometry with an excitation of 485 nm and emission wavelength of 528 nm and calculated using a standard curve of BSA. Plates were read on a BioTek Synergy 2 plate reader.

### Cytokine analyses.

For protein analysis, tissue was homogenized using a mini-beadbeater (BioSpec Products Inc.) for 1 min in a buffer containing 20 nM Tris HCl (pH 7.5), 150 nM NaCl, and 0.05% Tween 20 with Halt protease inhibitors (ThermoFisher Scientific). 1 ml of buffer was added per 100 mg of tissue. The samples were centrifuged to remove debris and supernatant was collected for analysis. Protein concentration was determined using DC

Protein Concentration Assay (BioRad). Cytokine concentrations were determined using Milliplex MAP Kit Mouse Th17 Magnetic Bead Panel (Cat # MTH17MAG-47K) according to manufacturer instructions. The plates were read using Magpix (Luminex). Cytokines in cell culture supernatants were measured using BioLegend ELISA Max deluxe kits for IL-1β (432604) and IL-23 (433704) according to manufacturer's instructions.

### Flow cytometry.

Mice were euthanized, and colons were removed, flushed with cold PBS, opened lengthwise and cut into 1 cm pieces. Colon pieces were incubated in HBSS buffer (supplemented with 15 mM HEPES, 5 mM EDTA, 1.25 mM DTT and 10% bovine calf serum) for 20 min at RT, then vortexed in PBS to remove epithelial cells. The HBSS wash step was repeated, and then tissue was vortexed in PBS three times. Tissue pieces were placed in R10 (RPMI 1640 supplemented with 10% FBS, L-glutamine, and penicillin/streptomycin) with 0.5 mg/ml collagenase VIII (Sigma) and placed in a shaking incubator at 37°C for 15 min. Samples were shaken by hand and filtered through 100 μm strainers on ice. Cells were washed with 35 ml cold R10, centrifuged at 400g for 10 min, then resuspended in FACS buffer (PBS with 2 mM EDTA and 1% FBS). 1–2 million cells were incubated with FACS buffer with 1% Fc block, 1% mouse serum, 1% rat serum, and 1% hamster serum, then stained with fluorophore conjugated antibodies against: CD45 (30-F11), Ly-6C (HK1.4), Ly-6G (1A8), CD103 (2E7), CX3CR1 (SA011F1), CD11c (N418), CD11b (M1/70 and M1/70), Ly-71 (F4/80, BM8), CCR6 (29–21.17), NK1.1 (CD161c, PK136), KLRG1 (2F1), CD90.2 (30-H12), NKp46 (Ly-94/NCR1, 29A1.4). To identify ILC, cells with lineage markers were excluded by staining for CD3 (17A2), CD5 (53–7.3), B220 (RA3–6B2), CD19 (6D5), TCRβ (H57–597), TCRγδ (UC7–13D5). Live cells were identified by exclusion of Zombie NIR fixable viability dye (BioLegend). For intracellular staining, cells were passed through Percoll gradient to isolate lymphocytes. Cells were resuspended in 1 ml R10 and 1–2 million cells were plated in 1 ml R10 with 1 μl Brefeldin A (BioLegend) for 4 h. Cells were washed in FACS buffer, and stained with surface antibodies as described above. Cells were then fixed and permeabilized using FoxP3 fix/perm reagents (eBioscience) following the manufacturer's instructions and stained with antibodies against RORγt (BD2) and IL-22 (Poly5164) or isotype control (RTK2071). Flow cytometry was performed on a CytoFLEX S (Beckman Coulter) and data were analyzed using FlowJo (TreeStar Inc.).

### Western blot analyses.

Frozen samples were homogenized in 200 μl RIPA buffer (150 mM NaCl, 50 mM Tris pH 7.4, 0.1% SDS, 1% IGEPAL (Alfa Aesar), 0.5% DOC) with Halt protease inhibitors (ThermoFisher Scientific) per 10 mg of tissue and centrifuged for 15 min at 4°C at 21,130g. Supernatant was collected and diluted 1:10 in RIPA buffer, then mixed with an equal volume of 2× Laemmli buffer and heated to 100°C for 5 min. Antibodies specific for RBCK1 (Santa Cruz Biotechnology sc-393754), HOIP (VWR/Proteintech 16298–1-AP, SHARPIN (VWR/Proteintech 14626–1-AP), and actin (Sigma-Aldrich A5316) were diluted 1:1000 in 3% milk TBS-T (HOIP, SHARPIN, actin) or 5% milk TBS-T (RBCK1). Blots were imaged using a BioRad ChemiDock Imager.

### Statistical analyses.

Statistical significance was determined using GraphPad Prism 9 software as described in the figure legends.

## Results

### HOIL1 restricts *C. rodentium* intestinal growth and dissemination to systemic sites.

While C57BL/6 mice exhibit mild symptoms upon gastrointestinal infection with *C. rodentium*, HOIL1-deficiency confers susceptibility to infection with weight-loss beginning around six days, and lethality occurring between 10 and 15 days post-infection (dpi; (24)). To gain further insight into role of HOIL1 in protecting against *C. rodentium* pathogenesis, we measured *C. rodentium* shedding in stool and burdens in tissues over the course of infection. Elevated *C. rodentium* shedding in the stool of *Hoil1*$^{-/-}$ mice was detectable as early as 2 dpi and continued for as long as stool pellets were obtainable from the HOIL1-mutant mice (Fig. 1A). Consistently, increased *C. rodentium* CFU were detected in the cecal contents and attached to the cecal tissue by 24 h post-infection (hpi) (Fig. 1B). Colonization of the distal colon was similar in both groups of mice up to 8 dpi (Fig. 1C). While *C. rodentium* CFU were rarely detected in the spleen and liver of *Hoil1*$^{+/+}$ mice before 10 dpi, bacteria were detected in these tissues in almost all *Hoil1*$^{-/-}$ mice by 4 dpi (Fig. 1D–E).

We considered that the detection of *C. rodentium* CFU in the spleen and liver of *Hoil1*$^{-/-}$ mice could be due to increased dissemination of bacteria from the intestine, or due to failure to kill bacteria that have reached these sites. To determine whether HOIL1 is required to control *C. rodentium* replication at systemic sites, we by-passed the intestinal epithelial barrier by infecting mice i.p. with $10^7$ CFU *C. rodentium*. Burdens in the spleen and liver were comparable between *Hoil1*$^{+/+}$ and *Hoil1*$^{-/-}$ mice at 12 hpi and at 4 dpi (Fig. 1F–G), suggesting that HOIL1 is not required to control *C. rodentium* replication outside the intestine. However, by 4 dpi, *Hoil1*$^{-/-}$ mice infected i.p. were shedding large amounts of *C. rodentium* in the stool indicating that infection of the GI tract had occurred in these mice (Fig. 1G), and that later time points would be uninformative. Together, these data indicate that HOIL1 plays an important role in restricting intestinal replication of *C. rodentium*, as well as in preventing its dissemination to systemic organs.

Since the previous experiments suggested that HOIL1 regulates intestinal barrier function, we next examined the severity of intestinal pathology and colitis over the course of infection. Thirty percent of the uninfected *Hoil1*$^{-/-}$ mice exhibited neutrophils in the epithelium, lamina propria, or muscularis mucosae (Fig. 1H and 1I). By 6 dpi, all *Hoil1*$^{-/-}$ mice exhibited inflammation, and 25% of these mice had developed ulcers, whereas only superficial neutrophilic inflammation was observed in the colon of 25% of *Hoil1*$^{+/+}$ mice. By 10 dpi, *Hoil1*$^{+/+}$ mice developed characteristic acute colitis, consisting of increased crypt depth, depletion of goblet cells, infiltration of immune cells and edema. In contrast, *Hoil1*$^{-/-}$ mice developed severe colitis, including ulceration, transmural inflammation and, in some cases, epithelial denudement. Additionally, a larger proportion of the colon was inflamed in *Hoil1*$^{-/-}$ mice at both time points (Fig. 1I). These data indicate that HOIL1 expression

is essential to protect against excessive inflammation and ulceration of the colon during *C. rodentium* infection.

We next asked whether HOIL1-deficiency resulted in an increase in intestinal permeability. Since *C. rodentium* was detected in systemic organs of *Hoil1*$^{-/-}$ mice by 4 dpi, we expected that any changes in intestinal permeability responsible for bacterial translocation would be detectable by this time. Naïve mice, or mice infected for 4 d, were administered FITC-dextran (4000 molecular weight) by oral gavage, and the concentration of FITC in the serum measured 4 h later (Fig. 1J). However, we did not observe a significant difference in the amount of FITC-dextran present in the serum of *Hoil1*$^{+/+}$ and *Hoil1*$^{-/-}$ mice before or during *C. rodentium* infection, suggesting that HOIL1 does not be required to regulate intestinal permeability in the early phases of *C. rodentium* infection. However, since significant damage to the colonic epithelium of *Hoil1*$^{-/-}$ mice occurred by 6 dpi, it is likely that loss of barrier integrity contributes systemic dissemination in the later stages of infection.

Together, these data show that HOIL1 is essential to limit colonic inflammation and prevent dissemination of *C. rodentium* to systemic organs following infection. However, HOIL1 does not appear to regulate passive intestinal permeability at 4 dpi, at which time *C. rodentium* CFU are detectable in systemic organs, suggesting that HOIL1 prevents dissemination through an active mechanism in the early stages of infection.

## HOIL1 plays an important role in the innate immune response to *C. rodentium*.

We next sought to determine which cell types require HOIL1 expression to prevent *C. rodentium*-induced pathology. Both the innate and adaptive branches of the immune response are required to control, clear, and survive *C. rodentium* infection (17, 23). To test whether HOIL1 plays a predominant role in innate or adaptive immune responses, we challenged *Rag1*$^{-/-}$*Hoil1*$^{+/+}$ and *Rag1*$^{-/-}$*Hoil1*$^{-/-}$ mice lacking mature B and T cells with *C. rodentium*. As reported by others (23), *Rag1*$^{-/-}$*Hoil1*$^{+/+}$ mice began to lose weight around 12 dpi and succumbed to the infection between 18 and 22 dpi (Fig. 2A–B, top). However, *Rag1*$^{-/-}$*Hoil1*$^{-/-}$ mice lost weight and succumbed to the infection approximately 7 d earlier, and in a similar time frame to *Hoil1*$^{-/-}$ mice (Fig. 2A–B, bottom; (24)). Furthermore, *Rag1*$^{-/-}$*Hoil1*$^{-/-}$ mice shed significantly more *C. rodentium* in their stool than *Rag1*$^{-/-}$*Hoil1*$^{+/+}$ mice as early as 2 dpi (Fig. 2C), and exhibited higher titers in the colon and cecum at 6 dpi, similar to *Hoil1*$^{-/-}$ mice (Fig. 2D, Fig. 1A–C). By 6 dpi, *C. rodentium* was detected at systemic sites including the liver, spleen, and mesenteric lymph nodes (MLN) in *Rag1*$^{-/-}$*Hoil1*$^{-/-}$ mice, while bacteria were rarely found outside the colon and cecum in *Rag1*$^{-/-}$*Hoil1*$^{+/+}$ mice at this time point (Fig. 2D). Although these data do not rule out a role for HOIL1 in the adaptive immune response to *C. rodentium*, they demonstrate that HOIL1 plays an essential role in the early innate immune response to *C. rodentium* in the absence of adaptive immunity.

## Expression of HOIL1 in radiation-resistant cells is important during *C. rodentium* infection.

Both hematopoietic cells and non-hematopoietic cells, such as intestinal epithelial cells (IEC), contribute to an effective innate immune response to *C. rodentium* infection in the intestine (23). To determine if HOIL1 is required in hematopoietic or non-hematopoietic

cells, we generated reciprocal bone marrow chimeric mice and allowed 16 weeks for bone marrow reconstitution and recovery from irradiation. Chimerism was confirmed by measuring the percent wild-type (WT) and knock-out (KO) gDNA in the blood (Fig. 3A). These mice were infected with *C. rodentium* and monitored for weight loss over 10 d (Fig. 3B). WT mice reconstituted with WT bone marrow (WT->WT) lost approximately 4% of their body weight over this time, indicating that 16 weeks was not sufficient for full recovery from irradiation. KO mice that received KO bone marrow (KO->KO) lost the greatest percentage of body weight (approximately 17%), as expected, and 50% of the mice succumbed before 10 dpi. WT mice that received KO bone marrow (KO->WT) lost approximately 8% of their body weight, indicating that loss of HOIL1 in bone marrow-derived cells only slightly increases susceptibility to *C. rodentium*-induced morbidity. KO mice that received WT bone marrow (WT->KO) exhibited delayed weight loss compared to KO->KO mice, but ultimately lost a similar percentage of body weight to the surviving KO->KO mice by 10 dpi. Thus, HOIL1 plays an important role in radiation-resistant cells during *C. rodentium* infection, although expression of HOIL1 in hematopoietic cells may be partially protective. These findings were further supported by increased *C. rodentium* CFU in the liver, and more severe pathology observed in colon from WT->KO mice relative to WT->WT mice at 10 dpi (Fig. 3C–D). Together, these data support a major role for HOIL1 in radiation-resistant cells to limit disease severity during *C. rodentium* infection, and a more minor role for HOIL1 in hematopoietic cells. Radiation-resistant cells include epithelial cells and stromal cells, as well as some long-lived hematopoietic cells present in tissues, such as macrophages and ILCs.

### HOIL1 is important in CD11c- and lysozyme-2-expressing cells to prevent systemic dissemination of *C. rodentium*.

To further identify which cell types require HOIL1 expression, we generated conditional knockout mice. Knock-out first mice with conditional potential were acquired from the European Mutant Mouse Archive (EMMA), and used to generate mice with exons 5 and 6 of the *Rbck1* gene, which encodes the HOIL1 protein, flanked by loxP sites. Deletion of these exons by crossing to mice expressing cre recombinase driven by the CMV promoter resulted in viable $Rbck1^{-/-}$ mice (herein referred to as such to distinguish them from the original $Hoil1^{-/-}$ mouse line), indicating that these mice are not fully LUBAC deficient similar to the $Hoil1^{-/-}$ mice. Indeed, HOIP and SHARPIN protein levels were reduced, but not completely absent in the spleen from $Rbck1^{-/-}$ mice (Suppl. Fig. 1A). *Rbck1* mRNA levels upstream of the deleted region were similar to wild-type levels (Suppl. Fig. 1B), indicating that the N-terminal region containing the ubiquitin-like domain important for complex formation may be expressed (43).

To confirm that $Rbck1^{-/-}$ mice displayed a similar phenotype to $Hoil1^{-/-}$ mice, we infected $Rbck1^{f/f}$ and $Rbck1^{-/-}$ mice with *C. rodentium*. Similar to $Hoil1^{-/-}$ mice (Fig. 2) (24), $Rbck1^{-/-}$ mice lost weight beginning around 6 dpi, and more than 50% succumbed to infection beginning at 10 dpi (Suppl. Fig. 1C–D). Weight loss in $Rbck1^{-/-}$ mice was slightly delayed compared to $Hoil1^{-/-}$ mice, and surviving mice recovered their body weight by 20 dpi. $Rbck1^{-/-}$ mice shed more *C. rodentium* in their stool early in infection (Suppl. Fig. 1E), and their colons were colonized more rapidly by *C. rodentium* compared to $Rbck1^{f/f}$

mice (Suppl. Fig. 1F). Furthermore, *C. rodentium* spread to systemic organs including the liver and spleen in *Rbck1*$^{-/-}$ mice (Suppl. Fig. 1G), although with slightly delayed kinetics compared to *Hoil1*$^{-/-}$ mice (Fig. 1D–E). Overall, these data indicate that *Rbck1*$^{-/-}$ mice have a similar phenotype to *Hoil1*$^{-/-}$ mice and are an appropriate model to examine the role of HOIL1 in specific cell types.

Since the susceptibility of the bone marrow chimeric mice to infection indicated that a radiation-resistant cell type was important, we hypothesized that HOIL1 expression may be required in intestinal epithelial cells (IECs), which are the primary site of *C. rodentium* infection. However, no differences were observed in the weight loss or bacterial shedding in the stool of *Rbck1*$^{f/-}$ and *Rbck1*$^{f/-\,\text{Vil1cre}}$ littermates over the course of infection (Fig. 4A, Suppl. Fig. 1I), and the colon was colonized to similar levels at 6 and 8 dpi (Fig. 4B). *C. rodentium* CFU were rarely detected in the liver, spleen, or MLN of *Rbck1*$^{f/-}$ or *Rbck1*$^{f/-\,\text{Vil1-cre}}$ mice at 6 or 8 dpi (Fig. 4C–D, Suppl. Table I). We confirmed efficient deletion of *Rbck1* in IECs by qRT-PCR (Suppl. Fig. 1H). These data indicate that HOIL1 is not required in IECs to control *C. rodentium* infection.

Additional innate cell types critical for the early response to *C. rodentium* infection include DCs, macrophages and neutrophils, which exhibit bactericidal activity and produce cytokines and chemokines that are important to initiate the immune response and limit pathogenesis during infection (14, 17, 52–54). We therefore examined if HOIL1 is required in CD11c- or lysozyme 2-expressing cells to prevent severe pathology following *C. rodentium* infection. Compared to *Rbck1*$^{f/-}$ littermates, *Rbck1*$^{f/-\,\text{CD11c-cre}}$ mice exhibited reduced body weight starting around 6–8 dpi and peaking at 14 dpi, but recovered by 18 dpi (Fig. 4E). No difference was observed in bacterial shedding in the stool, but *C. rodentium* colonized the colon more rapidly in *Rbck1*$^{f/-\,\text{CD11c-cre}}$ mice compared to *Rbck1*$^{f/-}$ mice (Fig. 4F, Suppl. Fig. 1J). Furthermore, *C. rodentium* CFU were detected in systemic organs of 23% of *Rbck1*$^{f/-\,\text{CD11c-cre}}$ mice by 4 dpi and approximately 40% by 8 dpi (Fig. 4G–H, Suppl. Table I). These data indicate that HOIL1 plays an important role in CD11c$^{+}$ mononuclear phagocytes to limit systemic dissemination and morbidity during infection.

*Rbck1*$^{f/-\,\text{Lyz2-cre}}$ mice also exhibited reduced body weight relative to their *Rbck1*$^{f/-}$ littermates starting around 8 dpi and peaking at 10 dpi, but recovered by 18 dpi (Fig. 4I). *Rbck1*$^{f/-\,\text{Lyz2-cre}}$ mice and *Rbck1*$^{f/-}$ mice shed similar amounts of bacteria early in infection, and *C. rodentium* burdens were similar in intestinal tissue (Fig. 4J, Suppl. Fig. 1K). We detected *C. rodentium* CFU in systemic organs of approximately 62.5% of *Rbck1*$^{f/-\,\text{Lyz2-cre}}$ mice at 8 dpi (Fig. 4K–L, Suppl. Table I). These data indicate that HOIL1 plays a role in lysozyme 2-expressing cells to control *C. rodentium* dissemination and limit morbidity. Lysozyme 2-expressing cells include macrophages and neutrophils that may be important for bacterial phagocytosis and clearance, as well as production of cytokines and chemokines.

Overall, these data indicate that HOIL1 functions in CD11c- and lysozyme-expressing myeloid cells to limit morbidity and systemic dissemination of bacteria following *C. rodentium* infection. However, the morbidity observed for *Rbck1*$^{f/-\,\text{CD11c-cre}}$ and *Rbck1*$^{f/-\,\text{Lyz2-cre}}$ mice was mild compared to *Rbck1*$^{-/-}$ mice, indicating that additional cell types are also involved.

### HOIL1 modulates the induction of IL-22 in the colon during *C. rodentium* infection

Since HOIL1 expression was required, at least in part, in myeloid cells, we examined whether HOIL1 deficiency results in defects or delays in induction of inflammatory cytokines produced by myeloid cells in response to *C. rodentium* infection that could allow the bacteria to replicate and colonize the colon more rapidly. We have shown previously that *Hoil1*$^{-/-}$ mice mount a defective type 1 inflammatory response, including impaired induction of IL-12, IFN-γ and iNOS, following *L. monocytogenes* infection (24). Since type 3 inflammatory cytokines IL-23 and IL-22 are an essential component of the mucosal innate immune response to *C. rodentium* (17, 19, 55–57), and IL-12 and IL-23 share subunit IL-12p40, we considered that HOIL1 may be required for induction of IL-23, and subsequently IL-22 and downstream responses. However, *Il12b* and *Il23a* mRNA levels changed minimally during 8 d of *C. rodentium* infection, and were not significantly different between *Hoil1*$^{+/+}$ and *Hoil1*$^{-/-}$ mice (Fig. 5A). Changes in IL-23 and IL-1β protein expression at 6 dpi were also minor (Fig. 5B). However, *Il22* mRNA and IL-22 protein were significantly lower in *Hoil1*$^{-/-}$ distal colon relative to *Hoil1*$^{+/+}$ tissue at 6 dpi (Fig. 5C).

We considered that IL-23 and IL-1β, which induce IL-22 production by ILC3, would likely be induced during the first few hours or days of infection while *C. rodentium* burdens were still low, and consequently that their induction might be too low to be detectable in whole tissue. Therefore, we treated bone marrow-derived DCs (BMDCs) and macrophages (BMDMs) with *C. rodentium* and measured expression of IL-23 and IL-1β. BMDCs rapidly and transiently secreted IL-23, and BMDMs secreted IL-1β with slightly delayed kinetics (Fig. 5D–E). However, *Hoil1*$^{-/-}$ cells secreted approximately half as much IL-23 and IL-1β at all time points. *Il23a* and *Il12b* mRNAs were induced similarly up to 3–4 hpi, but were lower in *Hoil1*$^{-/-}$ BMDCs at 6–10 hpi, while *Il1b* mRNA was significantly lower in *Hoil1*$^{-/-}$ BMDMs at all time points measured over 10 h (Fig. 5F–G). Although BMDCs and BMDMs are not identical to colonic DCs and macrophages, these data indicate that reduced induction of IL-23 and IL-1β by these cells may contribute to the impaired IL-22 induction observed in *Hoil1*$^{-/-}$ colon.

Chemokines are important for the recruitment of innate immune effector cells such as neutrophils and inflammatory monocytes to the site of infection. *Cxcl1* mRNA was lower in *Hoil1*$^{-/-}$ mice at 4 dpi (Fig. 5H), and CCL20 protein, which recruits CCR6-expressing cells such as ILC3 subsets, was slightly lower at baseline and significantly reduced during infection (Fig. 5I), indicating that recruitment of immune cells may also be impaired.

Since the LUBAC regulates type 1 inflammation (24, 26, 28, 40), and histological examination had indicated increased ulceration in *Hoil1*$^{-/-}$ colon during infection, we considered that type 1 inflammatory cytokines might also be dysregulated. Although *Il6, Tnf*, and *Ifng* mRNAs were induced similarly in *Hoil1*$^{+/+}$ and *Hoil1*$^{-/-}$ colon tissue, IL-6 protein was elevated at 6 dpi, IL-6 and TNF-α were significantly higher in uninfected *Hoil1*$^{-/-}$ tissue, suggesting that a low level of type 1 inflammation may be present in the colon of naïve *Hoil1*$^{-/-}$ mice (Fig. 5J–L).

Overall, we observed a reduction in IL-22 and CCL20 production in *Hoil1*$^{-/-}$ colon during infection, as well as a slight increase in IL-6 and TNF-α prior to infection. These data

indicate that HOIL1 modulates a subset of inflammatory cytokines in the colon during infection that could impair the anti-bacterial response.

## HOIL1 is important for ILC3 expansion and production of IL-22 during *C. rodentium* infection

Since expression of IL-22 and several chemokines were reduced in the colon of *Hoil1*$^{-/-}$ mice during infection, we next quantified innate immune cells in the colonic lamina propria by flow cytometry. Although numbers of neutrophils, monocytes and some DC subsets were increased at 6 dpi, no differences were observed between *Hoil1*$^{+/+}$ and *Hoil1*$^{-/-}$ tissue, except a small increase in the number of neutrophils in *Hoil1*$^{-/-}$ tissue during infection (Fig. 6A–D, Suppl. Fig. 2A–C). These data indicate that HOIL1 is not required for the maintenance or recruitment of neutrophils, resident macrophages, monocytes or DCs during *C. rodentium* infection.

We have recently shown that *Hoil1*$^{-/-}$ mice have increased numbers of ILC2 in the small intestine (45), so we considered that the impaired immune response to *C. rodentium* infection could be the result of altered ILC populations in the colon. ILC2 were also increased in the colon of naïve *Hoil1*$^{-/-}$ mice, although ILC1 and CCR6$^{+}$ ILC3 cells were unchanged (Fig. 6E–G, Suppl. Fig. 2E–F). Consistently, the type 2 inflammatory cytokine, *Il13*, was elevated in colon tissue from naïve *Hoil1*$^{-/-}$ mice (Suppl. Fig. 3A). Since IL-13 can induce significant changes to the cellular composition and function of the intestinal epithelium (58), we wondered whether IL-13-dependent changes to the intestinal epithelium might contribute to the susceptibility of *Hoil1*$^{-/-}$ mice to *C. rodentium*. To test this hypothesis, we used *Hoil1*$^{-/-}$ mice crossed to *Il4ra*$^{f/f}$ and Vil1-cre transgenic mice to block IL-13 signaling through the IL-4Rα selectively on intestinal epithelial cells (45). However, both *Hoil1*$^{-/-}$*Il4ra*$^{f/f}$ and *Hoil1*$^{-/-}$*Il4ra*$^{\Delta IEC}$ mice lost weight starting around 6 dpi, and succumbed to the infection between 10 and 15 dpi, whereas both *Hoil1*$^{+/+}$*Il4ra*$^{\Delta IEC}$ and *Hoil1*$^{+/+}$*Il4ra*$^{f/f}$ survived with infection to at least 21 dpi with minimal weight loss (Suppl. Fig. 3B,C). Furthermore, *Hoil1*$^{-/-}$*Il4ra*$^{\Delta IEC}$ and *Hoil1*$^{-/-}$*Il4ra*$^{f/f}$ mice both shed more *C. rodentium* CFU in their stool at 2 dpi, and experienced increased systemic dissemination at 6 dpi relative to *Hoil1*$^{+/+}$*Il4ra*$^{\Delta IEC}$ and *Hoil1*$^{+/+}$*Il4ra*$^{f/f}$ littermates (Suppl. Fig. 3D–E). These data indicate that the alterations in IEC differentiation caused by elevated IL-13 expression by ILC2 are not responsible for the increased replication, shedding and dissemination of *C. rodentium*, or morbidity observed in *Hoil1*$^{-/-}$ mice, although they do not rule out the possibility that elevated type 2 cytokines impact the functions of other cell types, such as macrophages.

Further analysis of the colonic ILC3 populations revealed that total RORγt$^{+}$ ILC3 and the proportion of RORγt$^{+}$ ILC3 expressing IL-22 increased in the colon of *Hoil1*$^{+/+}$ mice during infection, as expected (Fig. 6H–I, Suppl. Fig. 2G). However, these responses were significantly impaired in *Hoil1*$^{-/-}$ colon, resulting in approximately two thirds fewer IL-22$^{+}$ RORγt$^{+}$ ILC3 (Fig. 6H–J, Suppl. Fig. 2G), consistent with the 2–3-fold reduction in IL-22 protein expression. Together, these data indicate that HOIL1 is important to regulate both the number of ILC3 and IL-22 expression by ILC3 in the colon during *C. rodentium* infection,

and that a significant reduction in the number of IL-22$^{+}$ ILC3 in the intestine of *Hoil1*$^{-/-}$ mice may result in morbidity and mortality.

## Discussion

In this study, we provide insight into the role of LUBAC component, HOIL1, during bacterial infection of the gastrointestinal tract. We showed that HOIL1 is required to restrict early *C. rodentium* replication, dissemination to systemic organs and damage to the colonic epithelium. HOIL1 functioned in the innate response to prevent morbidity and mortality, and partly in CD11c- and lysozyme M-expressing cells. The increased susceptibility of *Hoil1*-mutant mice was associated with a reduction in the number of colonic ILC3s and impaired induction of IL-22 during infection, indicating that HOIL1 is an important regulator of the type 3 inflammatory response. These findings are biologically relevant since HOIL1-deficient patients experience recurrent colitis and increased susceptibility to bacterial infections, including *E. coli* (40).

Production of IL-22 by ILC3s is critical during the first few days of *C. rodentium* infection (17, 19, 55–57). IL-22-deficient or –depleted mice lose weight and succumb to infection in a similar time frame to *Hoil1*$^{-/-}$ mice, and exhibit increased *C. rodentium* burdens by 3–5 dpi, as well as dissemination to systemic organs (17–19). Although IL-22 production by T cells contributes to protection and clearance during the later stages of infection, mice lacking T cells or both T and B cells succumb to infection approximately one week later (18, 19, 23, 57). These studies support the conclusion that HOIL1 contributes to an effective innate immune response to *C. rodentium* by promoting ILC3 activation and production of IL-22.

Mechanistically, our data indicate that HOIL1 functions, at least in part, in myeloid cells to promote efficient upregulation of cytokines such as IL-23 and IL-1β that stimulate ILC3 expansion and production of IL-22 (16–19). Consistently, *Il23*$^{-/-}$ and *Il1r1*$^{-/-}$ mice are also highly susceptible to *C. rodentium* infection (15, 17, 18). Although we detected very little induction of these cytokines in the colon over the first four days of infection, likely due to low or variable colonization of the distal colon, our *in vitro* cytokine expression data and the early disease phenotypes of mice deficient in IL-23, IL-1R1, IL-22 or HOIL1 indicate that these cytokines are induced rapidly and function within this early window.

HOIL1 is a component of the LUBAC that generates linear polyubiquitin chains needed for NF-κB activation and transcription of type 1 inflammatory cytokines downstream of MyD88-dependent pathways as well as TNF family receptors (25–29, 32–34, 59). Our data indicate that HOIL1 and the LUBAC also regulate type 3 cytokine expression downstream of pattern recognition receptor activation. Additional studies will be required to identify the specific pathways involved, and determine whether HOIL1 or HOIP E3 ligase activity is required for ILC3 function and protection during infection. While HOIP generates linear ubiquitin chains, the physiological functions of HOIL1 ligase activity are less well understood (38, 39). *Myd88*$^{-/-}$ mice are similarly susceptible to *C. rodentium*, suggesting that the generation of linear ubiquitin chains by HOIP downstream of MyD88 may be important (60–64). MyD88 functions downstream of most TLRs as well as the IL-1 receptor family, and TLR2-deficiency is also detrimental during *C. rodentium* infection, although

TLR4-deficiency appears to be protective due to reduced intestinal inflammation (65–67). The IL-1R is also important, particularly on ILC3 and on IECs for the induction of IL-22 and response to IL-22, respectively, as well as the induction of chemokines, such as CCL20 (15, 16, 68, 69). However, the phenotypes of *Myd88*$^{-/-}$ and *Hoil1*$^{-/-}$ mice are not identical: hyperplasia is almost completely absent in *Myd88*$^{-/-}$ mice, but apparent in *Hoil1*$^{-/-}$ mice; and we observed that HOIL1 was more important in radiation-resistant cells, whereas MyD88 is more important in bone marrow-derived cells (60, 61). These findings indicate that HOIL1 and LUBAC activity may be required in additional signaling pathways.

The requirement for HOIL1 in myeloid cells is consistent with the importance of subsets of DCs, monocytes, macrophages and neutrophils in limiting *C. rodentium*-induced weight loss and systemic dissemination through their production of cytokines and bactericidal activities (14, 52–54, 60, 70, 71). However, loss of HOIL1 in myeloid cells or in bone marrow-derived cells only resulted in mild disease during infection, whereas loss of HOIL1 in radiation-resistant cells was significantly more detrimental, indicating that other cell types are also important. Radiation-resistant cells include IECs and stromal cells, but also some populations of resident immune cells, such as ILCs and macrophages. Despite IECs being the main cell type exposed to and infected by *C. rodentium*, loss of HOIL1 in IECs had no impact on the outcome of infection. It is likely that HOIL1 plays important roles in multiple cell types during *C. rodentium* infection. Future studies will be needed to test the requirement for HOIL1 expression in other cell types, such as ILC3, or in multiple cell types.

Overall, we have found that HOIL1 and the LUBAC play an important role in promoting a type 3 inflammatory response during intestinal infection with an attaching and effacing bacterial pathogen. Type 3 responses are critical for controlling other bacterial pathogens, such as EPEC and *Salmonella*, as well as for modulating responses to the commensal microbiota. These findings may also be relevant to IBD, where translocation of commensal microbes may be increased (72). A more thorough understanding of these mechanisms may aid in the development of therapeutics for gastrointestinal bacterial infections and inflammatory disorders.

## Supplementary Material

Refer to Web version on PubMed Central for supplementary material.

## Acknowledgements

We would like to thank D. Kreamalmeyer, M. White, X. Zhang, J. Marshall, M. Byrne, S. Madathil (Millipore), the UIC Research Resources Center Histology and Tissue Imaging Core and the Flow Cytometry Core, and the Digestive Diseases Research Core Center and the Developmental Biology Histology Core at Washington University for technical assistance. We thank members of the MacDuff laboratory and Skip Virgin's laboratory for helpful discussions, and B. Vallance for helpful suggestions. We thank Center d'ImmunoPhenomique (Ciphe) for providing the mutant mouse line (Allele: Rbck1$^{tm1a(EUCOMM)Hmgu}$), INFRAFRONTIER/EMMA (www.infrafrontier.eu, PMID: 25414328), and Institut de Transgenose (INTRAGENE, Orleans, France) from which the mouse line was distributed (EM:09852) (46, 47). Associated primary phenotypic information may be found at www.mousephenotype.org.

This work was funded in part by UIC institutional start-up funds and by NIAID R01 AI150640 to D.A.M.

## Abbreviations used:

| | |
|---|---|
| **C. rodentium** | Citrobacter rodentium |
| **HOIL1** | heme-oxidized IRP2 ubiquitin ligase-1 |
| **RBCK1** | RANBP2-type and C3HC4-type zinc finger containing 1 |
| **HOIP** | HOIL1 interacting protein |
| **SHARPIN** | SHANK-associated RH domain interacting protein |
| **LUBAC** | Linear Ubiquitin Chain Assembly Complex |
| **ILC** | innate lymphoid cell |
| **EPEC** | enteropathogenic *E. coli* |
| **EHEC** | enterohemorrhagic *E. coli* |
| **IEC** | intestinal epithelial cell |
| **IBD** | inflammatory bowel disease |
| **DC** | dendritic cell |
| **hpi** | hours post-infection |
| **dpi** | days post-infection |
| **LTi** | lymphoid tissue inducer cell |
| **RORγt** | RAR-related orphan receptor gamma |
| **i.g.** | intragastric |
| **BMDM** | bone marrow-derived macrophage |
| **BMDC** | bone marrow-derived dendritic cell |
| **LOD** | limit of detection |

## References

1. Liu L, Johnson HL, Cousens S, Perin J, Scott S, Lawn JE, Rudan I, Campbell H, Cibulskis R, Li M, Mathers C, and Black RE. 2012. Global, regional, and national causes of child mortality: an updated systematic analysis for 2010 with time trends since 2000. The Lancet 379: 2151–2161.
2. Nataro JP, and Kaper JB. 1998. Diarrheagenic Escherichia coli. Clin Microbiol Rev 11: 142–201. [PubMed: 9457432]
3. Levine MM, and Edelman R. 1984. Enteropathogenic Escherichia coli of classic serotypes associated with infant diarrhea: epidemiology and pathogenesis. Epidemiol Rev 6: 31–51. [PubMed: 6386503]
4. Croxen MA, Law RJ, Scholz R, Keeney KM, Wlodarska M, and Finlay BB. 2013. Recent advances in understanding enteric pathogenic Escherichia coli. Clin Microbiol Rev 26: 822–880. [PubMed: 24092857]

5. Denham JD, Nanjappa S, and Greene JN. 2018. Treatment of Enteropathogenic Escherichia coli Diarrhea in Cancer Patients: A Series of Three Cases. Case Rep Infect Dis 2018: 8438701. [PubMed: 29850308]

6. Nataro JP, and Kaper JB. 1998. Diarrheagenic Escherichia coli Clinical Microbiology Reviews 11: 142–201. [PubMed: 9457432]

7. Mundy R, MacDonald TT, Dougan G, Frankel G, and Wiles S. 2005. Citrobacter rodentium of mice and man. Cell Microbiol 7: 1697–1706. [PubMed: 16309456]

8. Luperchio SA, and Schauer DB. 2001. Molecular pathogenesis of Citrobacter rodentium and transmissible murine colonic hyperplasia. Microbes Infect 3: 333–340. [PubMed: 11334751]

9. Berger CN, Crepin VF, Roumeliotis TI, Wright JC, Carson D, Pevsner-Fischer M, Furniss RCD, Dougan G, Dori-Bachash M, Yu L, Clements A, Collins JW, Elinav E, Larrouy-Maumus GJ, Choudhary JS, and Frankel G. 2017. Citrobacter rodentium Subverts ATP Flux and Cholesterol Homeostasis in Intestinal Epithelial Cells In Vivo. Cell Metab 26: 738–752 e736. [PubMed: 28988824]

10. Berger CN, Crepin VF, Roumeliotis TI, Wright JC, Serafini N, Pevsner-Fischer M, Yu L, Elinav E, Di Santo JP, Choudhary JS, and Frankel G. 2018. The Citrobacter rodentium type III secretion system effector EspO affects mucosal damage repair and antimicrobial responses. PLoS Pathog 14: e1007406.

11. Wong AR, Pearson JS, Bright MD, Munera D, Robinson KS, Lee SF, Frankel G, and Hartland EL. 2011. Enteropathogenic and enterohaemorrhagic Escherichia coli: even more subversive elements. Mol Microbiol 80: 1420–1438. [PubMed: 21488979]

12. Eckmann L 2006. Animal models of inflammatory bowel disease: lessons from enteric infections. Ann N Y Acad Sci 1072: 28–38. [PubMed: 17057188]

13. Wiles S, Clare S, Harker J, Huett A, Young D, Dougan G, and Frankel G. 2004. Organ specificity, colonization and clearance dynamics in vivo following oral challenges with the murine pathogen Citrobacter rodentium. Cell Microbiol 6: 963–972. [PubMed: 15339271]

14. Aychek T, Mildner A, Yona S, Kim KW, Lampl N, Reich-Zeliger S, Boon L, Yogev N, Waisman A, Cua DJ, and Jung S. 2015. IL-23-mediated mononuclear phagocyte crosstalk protects mice from Citrobacter rodentium-induced colon immunopathology. Nat Commun 6: 6525. [PubMed: 25761673]

15. Lebeis SL, Powell KR, Merlin D, Sherman MA, and Kalman D. 2009. Interleukin-1 receptor signaling protects mice from lethal intestinal damage caused by the attaching and effacing pathogen Citrobacter rodentium. Infect Immun 77: 604–614. [PubMed: 19075023]

16. Reynders A, Yessaad N, Vu Manh TP, Dalod M, Fenis A, Aubry C, Nikitas G, Escaliere B, Renauld JC, Dussurget O, Cossart P, Lecuit M, Vivier E, and Tomasello E. 2011. Identity, regulation and in vivo function of gut NKp46+RORgammat+ and NKp46+RORgammat- lymphoid cells. EMBO J 30: 2934–2947. [PubMed: 21685873]

17. Zheng Y, Valdez PA, Danilenko DM, Hu Y, Sa SM, Gong Q, Abbas AR, Modrusan Z, Ghilardi N, de Sauvage FJ, and Ouyang W. 2008. Interleukin-22 mediates early host defense against attaching and effacing bacterial pathogens. Nat Med 14: 282–289. [PubMed: 18264109]

18. Basu R, O'Quinn DB, Silberger DJ, Schoeb TR, Fouser L, Ouyang W, Hatton RD, and Weaver CT. 2012. Th22 cells are an important source of IL-22 for host protection against enteropathogenic bacteria. Immunity 37: 1061–1075. [PubMed: 23200827]

19. Sonnenberg GF, Monticelli LA, Elloso MM, Fouser LA, and Artis D. 2011. CD4(+) lymphoid tissue-inducer cells promote innate immunity in the gut. Immunity 34: 122–134. [PubMed: 21194981]

20. Liang SC, Nickerson-Nutter C, Pittman DD, Carrier Y, Goodwin DG, Shields KM, Lambert AJ, Schelling SH, Medley QG, Ma HL, Collins M, Dunussi-Joannopoulos K, and Fouser LA. 2010. IL-22 induces an acute-phase response. J Immunol 185: 5531–5538. [PubMed: 20870942]

21. Liang SC, Tan XY, Luxenberg DP, Karim R, Dunussi-Joannopoulos K, Collins M, and Fouser LA. 2006. Interleukin (IL)-22 and IL-17 are coexpressed by Th17 cells and cooperatively enhance expression of antimicrobial peptides. J Exp Med 203: 2271–2279. [PubMed: 16982811]

22. Wolk K, Kunz S, Witte E, Friedrich M, Asadullah K, and Sabat R. 2004. IL-22 increases the innate immunity of tissues. Immunity 21: 241–254. [PubMed: 15308104]

23. Vallance BA, Deng W, Knodler LA, and Finlay BB. 2002. Mice lacking T and B lymphocytes develop transient colitis and crypt hyperplasia yet suffer impaired bacterial clearance during Citrobacter rodentium infection. Infect Immun 70: 2070–2081. [PubMed: 11895973]
24. MacDuff DA, Reese TA, Kimmey JM, Weiss LA, Song C, Zhang X, Kambal A, Duan E, Carrero JA, Boisson B, Laplantine E, Israel A, Picard C, Colonna M, Edelson BT, Sibley LD, Stallings CL, Casanova JL, Iwai K, and Virgin HW. 2015. Phenotypic complementation of genetic immunodeficiency by chronic herpesvirus infection. Elife 4: e04494. [PubMed: 25599590]
25. Kirisako T, Kamei K, Murata S, Kato M, Fukumoto H, Kanie M, Sano S, Tokunaga F, Tanaka K, and Iwai K. 2006. A ubiquitin ligase complex assembles linear polyubiquitin chains. EMBO J 25: 4877–4887. [PubMed: 17006537]
26. Tokunaga F, Sakata S, Saeki Y, Satomi Y, Kirisako T, Kamei K, Nakagawa T, Kato M, Murata S, Yamaoka S, Yamamoto M, Akira S, Takao T, Tanaka K, and Iwai K. 2009. Involvement of linear polyubiquitylation of NEMO in NF-kappaB activation. Nat Cell Biol 11: 123–132. [PubMed: 19136968]
27. Emmerich CH, Ordureau A, Strickson S, Arthur JS, Pedrioli PG, Komander D, and Cohen P. 2013. Activation of the canonical IKK complex by K63/M1-linked hybrid ubiquitin chains. Proc Natl Acad Sci U S A 110: 15247–15252. [PubMed: 23986494]
28. Haas TL, Emmerich CH, Gerlach B, Schmukle AC, Cordier SM, Rieser E, Feltham R, Vince J, Warnken U, Wenger T, Koschny R, Komander D, Silke J, and Walczak H. 2009. Recruitment of the linear ubiquitin chain assembly complex stabilizes the TNF-R1 signaling complex and is required for TNF-mediated gene induction. Mol Cell 36: 831–844. [PubMed: 20005846]
29. Hostager BS, Fox DK, Whitten D, Wilkerson CG, Eipper BA, Francone VP, Rothman PB, and Colgan JD. 2010. HOIL-1L interacting protein (HOIP) as an NF-kappaB regulating component of the CD40 signaling complex. PLoS One 5: e11380. [PubMed: 20614026]
30. Ikeda F, Deribe YL, Skanland SS, Stieglitz B, Grabbe C, Franz-Wachtel M, van Wijk SJ, Goswami P, Nagy V, Terzic J, Tokunaga F, Androulidaki A, Nakagawa T, Pasparakis M, Iwai K, Sundberg JP, Schaefer L, Rittinger K, Macek B, and Dikic I. 2011. SHARPIN forms a linear ubiquitin ligase complex regulating NF-kappaB activity and apoptosis. Nature 471: 637–641. [PubMed: 21455181]
31. Inn KS, Gack MU, Tokunaga F, Shi M, Wong LY, Iwai K, and Jung JU. 2011. Linear ubiquitin assembly complex negatively regulates RIG-I- and TRIM25-mediated type I interferon induction. Mol Cell 41: 354–365. [PubMed: 21292167]
32. Zak DE, Schmitz F, Gold ES, Diercks AH, Peschon JJ, Valvo JS, Niemisto A, Podolsky I, Fallen SG, Suen R, Stolyar T, Johnson CD, Kennedy KA, Hamilton MK, Siggs OM, Beutler B, and Aderem A. 2011. Systems analysis identifies an essential role for SHANK-associated RH domain-interacting protein (SHARPIN) in macrophage Toll-like receptor 2 (TLR2) responses. Proc Natl Acad Sci U S A 108: 11536–11541. [PubMed: 21709223]
33. Damgaard RB, Nachbur U, Yabal M, Wong WW, Fiil BK, Kastirr M, Rieser E, Rickard JA, Bankovacki A, Peschel C, Ruland J, Bekker-Jensen S, Mailand N, Kaufmann T, Strasser A, Walczak H, Silke J, Jost PJ, and Gyrd-Hansen M. 2012. The ubiquitin ligase XIAP recruits LUBAC for NOD2 signaling in inflammation and innate immunity. Mol Cell 46: 746–758. [PubMed: 22607974]
34. Rodgers MA, Bowman JW, Fujita H, Orazio N, Shi M, Liang Q, Amatya R, Kelly TJ, Iwai K, Ting J, and Jung JU. 2014. The linear ubiquitin assembly complex (LUBAC) is essential for NLRP3 inflammasome activation. J Exp Med 211: 1333–1347. [PubMed: 24958845]
35. Gurung P, Lamkanfi M, and Kanneganti TD. 2015. Cutting edge: SHARPIN is required for optimal NLRP3 inflammasome activation. J Immunol 194: 2064–2067. [PubMed: 25637014]
36. Hostager BS, Kashiwada M, Colgan JD, and Rothman PB. 2011. HOIL-1L interacting protein (HOIP) is essential for CD40 signaling. PLoS One 6: e23061. [PubMed: 21829693]
37. Kelsall IR, Zhang J, Knebel A, Arthur JSC, and Cohen P. 2019. The E3 ligase HOIL-1 catalyses ester bond formation between ubiquitin and components of the Myddosome in mammalian cells. Proc Natl Acad Sci U S A 116: 13293–13298. [PubMed: 31209050]
38. Fuseya Y, Fujita H, Kim M, Ohtake F, Nishide A, Sasaki K, Saeki Y, Tanaka K, Takahashi R, and Iwai K. 2020. The HOIL-1L ligase modulates immune signalling and cell death via monoubiquitination of LUBAC. Nat Cell Biol 22: 663–673. [PubMed: 32393887]

39. Kelsall IR, McCrory EH, Xu Y, Scudamore CL, Nanda SK, Mancebo-Gamella P, Wood NT, Knebel A, Matthews SJ, and Cohen P. 2022. HOIL-1 ubiquitin ligase activity targets unbranched glucosaccharides and is required to prevent polyglucosan accumulation. EMBO J 41: e109700. [PubMed: 35274759]

40. Boisson B, Laplantine E, Prando C, Giliani S, Israelsson E, Xu Z, Abhyankar A, Israel L, Trevejo-Nunez G, Bogunovic D, Cepika AM, MacDuff D, Chrabieh M, Hubeau M, Bajolle F, Debre M, Mazzolari E, Vairo D, Agou F, Virgin HW, Bossuyt X, Rambaud C, Facchetti F, Bonnet D, Quartier P, Fournet JC, Pascual V, Chaussabel D, Notarangelo LD, Puel A, Israel A, Casanova JL, and Picard C. 2012. Immunodeficiency, autoinflammation and amylopectinosis in humans with inherited HOIL-1 and LUBAC deficiency. Nat Immunol 13: 1178–1186. [PubMed: 23104095]

41. Boisson B, Laplantine E, Dobbs K, Cobat A, Tarantino N, Hazen M, Lidov HG, Hopkins G, Du L, Belkadi A, Chrabieh M, Itan Y, Picard C, Fournet JC, Eibel H, Tsitsikov E, Pai SY, Abel L, Al-Herz W, Casanova JL, Israel A, and Notarangelo LD. 2015. Human HOIP and LUBAC deficiency underlies autoinflammation, immunodeficiency, amylopectinosis, and lymphangiectasia. J Exp Med 212: 939–951. [PubMed: 26008899]

42. Oda H, Beck DB, Kuehn HS, Sampaio Moura N, Hoffmann P, Ibarra M, Stoddard J, Tsai WL, Gutierrez-Cruz G, Gadina M, Rosenzweig SD, Kastner DL, Notarangelo LD, and Aksentijevich I. 2019. Second Case of HOIP Deficiency Expands Clinical Features and Defines Inflammatory Transcriptome Regulated by LUBAC. Front Immunol 10: 479. [PubMed: 30936877]

43. Fujita H, Tokunaga A, Shimizu S, Whiting AL, Aguilar-Alonso F, Takagi K, Walinda E, Sasaki Y, Shimokawa T, Mizushima T, Ohki I, Ariyoshi M, Tochio H, Bernal F, Shirakawa M, and Iwai K. 2018. Cooperative Domain Formation by Homologous Motifs in HOIL-1L and SHARPIN Plays A Crucial Role in LUBAC Stabilization. Cell Rep 23: 1192–1204. [PubMed: 29694895]

44. Peltzer N, Darding M, Montinaro A, Draber P, Draberova H, Kupka S, Rieser E, Fisher A, Hutchinson C, Taraborrelli L, Hartwig T, Lafont E, Haas TL, Shimizu Y, Boiers C, Sarr A, Rickard J, Alvarez-Diaz S, Ashworth MT, Beal A, Enver T, Bertin J, Kaiser W, Strasser A, Silke J, Bouillet P, and Walczak H. 2018. LUBAC is essential for embryogenesis by preventing cell death and enabling haematopoiesis. Nature 557: 112–117. [PubMed: 29695863]

45. Wood MJ, Marshall JN, Hartley VL, Liu TC, Iwai K, Stappenbeck TS, and MacDuff DA. 2022. HOIL1 regulates group 2 innate lymphoid cell numbers and type 2 inflammation in the small intestine. Mucosal Immunol 15: 642–655. [PubMed: 35534698]

46. Consortium, I. 2015. INFRAFRONTIER--providing mutant mouse resources as research tools for the international scientific community. Nucleic Acids Res 43: D1171–1175. [PubMed: 25414328]

47. Raess M, de Castro AA, Gailus-Durner V, Fessele S, Hrabe de Angelis M, and I. Consortium. 2016. INFRAFRONTIER: a European resource for studying the functional basis of human disease. Mamm Genome 27: 445–450. [PubMed: 27262858]

48. Schauer DB, and Falkow S. 1993. Attaching and Effacing Locus of a Citrobacterfreundii Biotype That Causes Transmissible Murine Colonic Hyperplasia. Infection and Immunity 61. 2486–2492. [PubMed: 8500884]

49. Hwang S, Maloney NS, Bruinsma MW, Goel G, Duan E, Zhang L, Shrestha B, Diamond MS, Dani A, Sosnovtsev SV, Green KY, Lopez-Otin C, Xavier RJ, Thackray LB, and Virgin HW. 2012. Nondegradative role of Atg5-Atg12/ Atg16L1 autophagy protein complex in antiviral activity of interferon gamma. Cell Host Microbe 11: 397–409. [PubMed: 22520467]

50. MacDuff DA, Baldridge MT, Qaqish AM, Nice TJ, Darbandi AD, Hartley VL, Peterson ST, Miner JJ, Iwai K, and Virgin HW. 2018. HOIL1 Is Essential for the Induction of Type I and III Interferons by MDA5 and Regulates Persistent Murine Norovirus Infection. J Virol 92. e01368–18.

51. Yokoyama CC, Baldridge MT, Leung DW, Zhao G, Desai C, Liu TC, Diaz-Ochoa VE, Huynh JP, Kimmey JM, Sennott EL, Hole CR, Idol RA, Park S, Storek KM, Wang C, Hwang S, Viehmann Milam A, Chen E, Kerrinnes T, Starnbach MN, Handley SA, Mysorekar IU, Allen PM, Monack DM, Dinauer MC, Doering TL, Tsolis RM, Dworkin JE, Stallings CL, Amarasinghe GK, Micchelli CA, and Virgin HW. 2018. LysMD3 is a type II membrane protein without an in vivo role in the response to a range of pathogens. J Biol Chem 293: 6022–6038. [PubMed: 29496999]

52. Longman RS, Diehl GE, Victorio DA, Huh JR, Galan C, Miraldi ER, Swaminath A, Bonneau R, Scherl EJ, and Littman DR. 2014. CX(3)CR1(+) mononuclear phagocytes support colitis-

associated innate lymphoid cell production of IL-22. J Exp Med 211: 1571–1583. [PubMed: 25024136]

53. Satpathy AT, Briseno CG, Lee JS, Ng D, Manieri NA, Kc W, Wu X, Thomas SR, Lee WL, Turkoz M, McDonald KG, Meredith MM, Song C, Guidos CJ, Newberry RD, Ouyang W, Murphy TL, Stappenbeck TS, Gommerman JL, Nussenzweig MC, Colonna M, Kopan R, and Murphy KM. 2013. Notch2-dependent classical dendritic cells orchestrate intestinal immunity to attaching-and-effacing bacterial pathogens. Nat Immunol 14: 937–948. [PubMed: 23913046]
54. Schreiber HA, Loschko J, Karssemeijer RA, Escolano A, Meredith MM, Mucida D, Guermonprez P, and Nussenzweig MC. 2013. Intestinal monocytes and macrophages are required for T cell polarization in response to Citrobacter rodentium. J Exp Med 210: 2025–2039. [PubMed: 24043764]
55. Satoh-Takayama N, Vosshenrich CA, Lesjean-Pottier S, Sawa S, Lochner M, Rattis F, Mention JJ, Thiam K, Cerf-Bensussan N, Mandelboim O, Eberl G, and Di Santo JP. 2008. Microbial flora drives interleukin 22 production in intestinal NKp46+ cells that provide innate mucosal immune defense. Immunity 29: 958–970. [PubMed: 19084435]
56. Cella M, Fuchs A, Vermi W, Facchetti F, Otero K, Lennerz JK, Doherty JM, Mills JC, and Colonna M. 2009. A human natural killer cell subset provides an innate source of IL-22 for mucosal immunity. Nature 457: 722–725. [PubMed: 18978771]
57. Song C, Lee JS, Gilfillan S, Robinette ML, Newberry RD, Stappenbeck TS, Mack M, Cella M, and Colonna M. 2015. Unique and redundant functions of NKp46+ ILC3s in models of intestinal inflammation. J Exp Med 212: 1869–1882. [PubMed: 26458769]
58. McKenzie GJ, Bancroft A, Grencis RK, and McKenzie AN. 1998. A distinct role for interleukin-13 in Th2-cell-mediated immune responses. Curr Biol 8: 339–342. [PubMed: 9512421]
59. Zinngrebe J, Rieser E, Taraborrelli L, Peltzer N, Hartwig T, Ren H, Kovacs I, Endres C, Draber P, Darding M, von Karstedt S, Lemke J, Dome B, Bergmann M, Ferguson BJ, and Walczak H. 2016. --LUBAC deficiency perturbs TLR3 signaling to cause immunodeficiency and autoinflammation. J Exp Med 213: 2671–2689. [PubMed: 27810922]
60. Lebeis SL, Bommarius B, Parkos CA, Sherman MA, and Kalman D. 2007. TLR signaling mediated by MyD88 is required for a protective innate immune response by neutrophils to Citrobacter rodentium. J Immunol 179: 566–577. [PubMed: 17579078]
61. Gibson DL, Ma C, Bergstrom KS, Huang JT, Man C, and Vallance BA. 2008. MyD88 signalling plays a critical role in host defence by controlling pathogen burden and promoting epithelial cell homeostasis during Citrobacter rodentium-induced colitis. Cell Microbiol 10: 618–631. [PubMed: 17979981]
62. Bhinder G, Stahl M, Sham HP, Crowley SM, Morampudi V, Dalwadi U, Ma C, Jacobson K, and Vallance BA. 2014. Intestinal epithelium-specific MyD88 signaling impacts host susceptibility to infectious colitis by promoting protective goblet cell and antimicrobial responses. Infect Immun 82: 3753–3763. [PubMed: 24958710]
63. Cohen P, and Strickson S. 2017. The role of hybrid ubiquitin chains in the MyD88 and other innate immune signalling pathways. Cell Death Differ 24: 1153–1159. [PubMed: 28475177]
64. Friedrich C, Mamareli P, Thiemann S, Kruse F, Wang Z, Holzmann B, Strowig T, Sparwasser T, and Lochner M. 2017. MyD88 signaling in dendritic cells and the intestinal epithelium controls immunity against intestinal infection with C. rodentium. PLoS Pathog 13: e1006357. [PubMed: 28520792]
65. Khan MA, Ma C, Knodler LA, Valdez Y, Rosenberger CM, Deng W, Finlay BB, and Vallance BA. 2006. Toll-like receptor 4 contributes to colitis development but not to host defense during Citrobacter rodentium infection in mice. Infect Immun 74: 2522–2536. [PubMed: 16622187]
66. Gibson DL, Ma C, Rosenberger CM, Bergstrom KS, Valdez Y, Huang JT, Khan MA, and Vallance BA. 2008. Toll-like receptor 2 plays a critical role in maintaining mucosal integrity during Citrobacter rodentium-induced colitis. Cell Microbiol 10: 388–403. [PubMed: 17910742]
67. Gibson DL, Montero M, Ropeleski MJ, Bergstrom KS, Ma C, Ghosh S, Merkens H, Huang J, Mansson LE, Sham HP, McNagny KM, and Vallance BA. 2010. Interleukin-11 reduces TLR4-induced colitis in TLR2-deficient mice and restores intestinal STAT3 signaling. Gastroenterology 139: 1277–1288. [PubMed: 20600022]

68. Lee YS, Yang H, Yang JY, Kim Y, Lee SH, Kim JH, Jang YJ, Vallance BA, and Kweon MN. 2015. Interleukin-1 (IL-1) signaling in intestinal stromal cells controls KC/ CXCL1 secretion, which correlates with recruitment of IL-22- secreting neutrophils at early stages of Citrobacter rodentium infection. Infect Immun 83: 3257–3267. [PubMed: 26034212]

69. Overcast GR, Meibers HE, Eshleman EM, Saha I, Waggoner L, Patel KN, Jain VG, Haslam DB, Alenghat T, VanDussen KL, and Pasare C. 2023. IEC-intrinsic IL-1R signaling holds dual roles in regulating intestinal homeostasis and inflammation. J Exp Med 220. e20212523.

70. Wang Y, Koroleva EP, Kruglov AA, Kuprash DV, Nedospasov SA, Fu YX, and Tumanov AV. 2010. Lymphotoxin beta receptor signaling in intestinal epithelial cells orchestrates innate immune responses against mucosal bacterial infection. Immunity 32: 403–413. [PubMed: 20226692]

71. Manta C, Heupel E, Radulovic K, Rossini V, Garbi N, Riedel CU, and Niess JH. 2013. CX(3)CR1(+) macrophages support IL-22 production by innate lymphoid cells during infection with Citrobacter rodentium. Mucosal Immunol 6: 177–188. [PubMed: 22854708]

72. Schmitz H, Barmeyer C, Fromm M, Runkel N, Foss HD, Bentzel CJ, Riecken EO, and Schulzke JD. 1999. Altered tight junction structure contributes to the impaired epithelial barrier function in ulcerative colitis. Gastroenterology 116: 301–309. [PubMed: 9922310]

**Key Points**

- HOIL1 restricts early intestinal replication and systemic spread of *C. rodentium*.
- HOIL1 functions partly in myeloid cells to limit morbidity and systemic spread.
- HOIL1 promotes ILC3 expansion and IL-22 expression during *C. rodentium* infection.

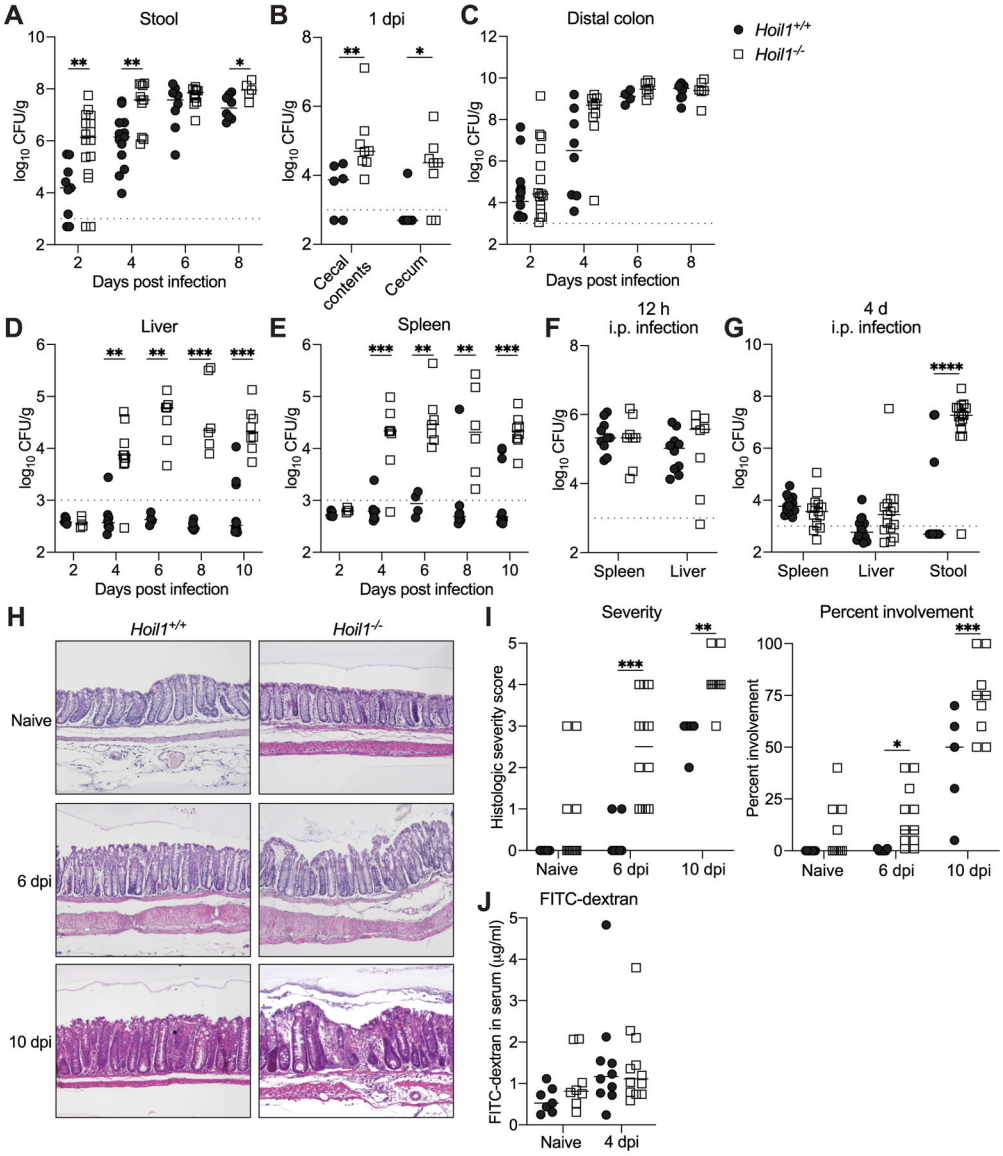


**Figure 1: HOIL1 prevents bacterial dissemination to systemic sites and colonic ulceration following *C. rodentium* infection.**

**A-E**. *C. rodentium* CFU in stool (A), cecal contents and cecum (B), distal colon (C), liver (D) and spleen (E) of *Hoil1*$^{+/+}$ (circles) and *Hoil1*$^{-/-}$ (squares) mice on indicated days following i.g. inoculation with $2\times10^9$ CFU *C. rodentium*. **F**. *C. rodentium* CFU in spleen and liver 12 h post-infection of *Hoil1*$^{+/+}$ and *Hoil1*$^{-/-}$ mice following i.p. inoculation with $10^7$ CFU. **G**. *C. rodentium* CFU in spleen, liver, and stool of *Hoil1*$^{+/+}$ and *Hoil1*$^{-/-}$ mice 4 d following i.p. inoculation with $10^7$ CFU. **H**. Representative H&E-stained sections of distal colon from naïve *Hoil1*$^{+/+}$ (left panels) and *Hoil1*$^{-/-}$ (right panels) mice (top), or mice inoculated i.g. with *C. rodentium* for 6 d (middle) or 10 d (bottom). **I**. Histological severity score (left) and percent of colon length involvement (right) of *Hoil1*$^{+/+}$ (circles) and *Hoil1*$^{-/-}$ (squares) mice 0, 6, and 10 d post-infection. Histological scoring criteria: 0, no neutrophilic inflammation; 1, neutrophilic inflammation in surface epithelium, lamina propria, or cryptitis; 2, crypt abscess; 3, neutrophilic inflammation present at muscularis mucosae or

beyond; 4, ulcer or transmural inflammation; 5, epithelium denudement. **J**. Concentration of FITC-dextran in serum 4 h after i.g. administration in *Hoil1*$^{+/+}$ and *Hoil1*$^{-/-}$ naïve mice, and at 4 d post-inoculation with $2\times10^9$ CFU *C. rodentium* i.g. Each symbol represents an individual mouse, and the median is indicated. Dotted line indicates limit of detection (LOD). Data were combined from at least 3 independent experiments. Statistical analyses were performed using Mann-Whitney test. *$p\leq0.05$, **$p\leq0.01$, ***$p\leq0.001$, ****$p\leq0.0001$.

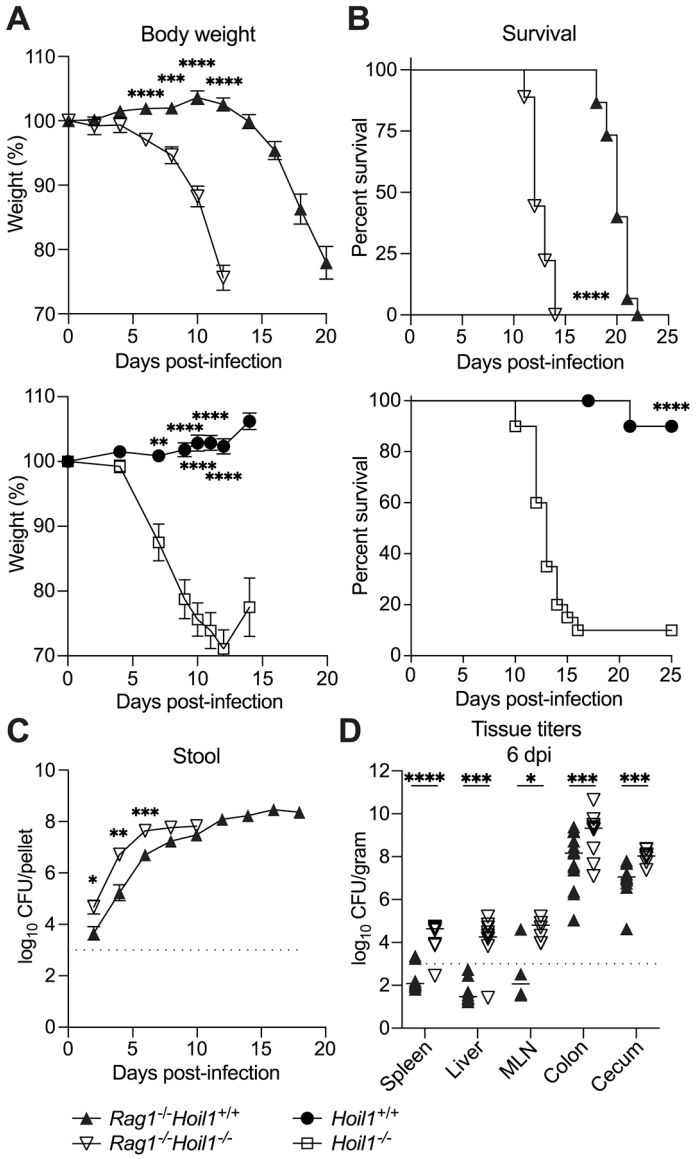


**Figure 2: HOIL1 functions in innate immunity during *C. rodentium* infection.**

**A**. Percent initial body weight of $Rag^{-/-}Hoil1^{+/+}$ (filled triangles; $n = 15$) and $Rag^{-/-}Hoil1^{-/-}$ (inverted triangles; $n = 9$) (top panel), and $Hoil1^{+/+}$ (filled circles; $n = 10$) and $Hoil1^{-/-}$ (squares; $n = 10$) (bottom panel) mice at the indicated times following i.g. inoculation with $2\times10^9$ CFU *C. rodentium*. **B**. Survival of $Rag^{-/-}Hoil1^{+/+}$ ($n = 15$) and $Rag^{-/-}Hoil1^{-/-}$ ($n = 9$) (top panel), and $Hoil1^{+/+}$ ($n = 20$) and $Hoil1^{-/-}$ ($n = 20$) (bottom panel) mice following i.g. inoculation with $2\times10^9$ CFU *C. rodentium*. **C**. *C. rodentium* CFU in stool from $Rag^{-/-}Hoil1^{+/+}$ ($n = 15$) and $Rag^{-/-}Hoil1^{-/-}$ ($n = 9$) mice at the indicated times following i.g. inoculation with $2\times10^9$ CFU *C. rodentium*. Data represent the mean ± SEM. **D**. *C. rodentium* CFU in spleen, liver, mesenteric lymph node (MLN), distal colon and cecum of $Rag^{-/-}Hoil1^{+/+}$ and $Rag^{-/-}Hoil1^{-/-}$ 6 dpi with $2\times10^9$ CFU *C. rodentium* i.g. Each symbol represents an individual mouse and bars indicate the median. Data in bottom panels of (A) and (B) reprinted from MacDuff *et. al.*, eLife 2015 (24). Dotted lines indicate the

LOD. Data were combined from at least three independent experiments. Statistical analyses performed using unpaired *t*-test with Welch correction (A), log-rank Mantel-Cox test (B), or Mann-Whitney test (C, D). *$p \leq 0.05$, **$p \leq 0.01$, ***$p \leq 0.001$, ****$p \leq 0.0001$.

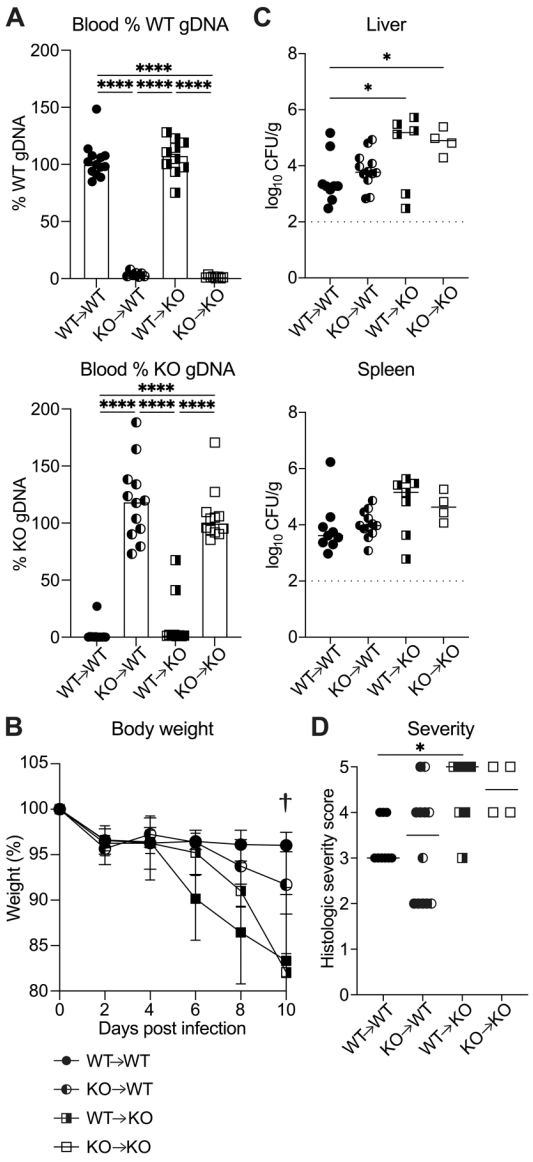


**Figure 3: HOIL1 is important in radiation-resistant cells during *C. rodentium* infection.**

**A.** Percent of WT (left panel) or KO (right panel) gDNA in blood from bone marrow chimeric mice relative to WT->WT and KO->KO controls. Each symbol represents an individual mouse and bars indicate the median. **B**. Percent of initial weight of *Hoil1* WT->WT ($n = 9$), *Hoil1* KO->WT ($n = 12$), *Hoil1* WT->KO ($n = 8$) and *Hoil1* KO->KO ($n = 8$) bone marrow chimeric mice over 10 d following i.g. inoculation with $2\times10^9$ CFU *C. rodentium*. Data represent the median ± interquartile range. Significant at 8 dpi: WT->WT vs KO->KO, KO->WT vs KO->KO, and WT->KO vs KO->KO. Significant at 10 dpi: WT->WT vs KO->KO, WT->WT vs WT->KO, WT->KO vs KO->WT, and KO->WT vs KO->KO. † 4 of 8 KO->KO mice died between 8 and 10 dpi. **C.** *C. rodentium* CFU in liver and spleen at 10 dpi. **D.** Histologic severity score for colon at 10 dpi. For A, C, D, each symbol represents an individual mouse, and bars indicate the median. Data were combined from at least 3 independent experiments. Statistical analyses performed by Brown-Forsythe

and Welch one-way ANOVA with Dunnett's T3 multiple comparisons test (A and D), two-way ANOVA with Tukey's multiple comparisons test (B), one-way ANOVA relative to WT->WT (C). *$p \leq 0.05$, ****$p \leq 0.0001$.

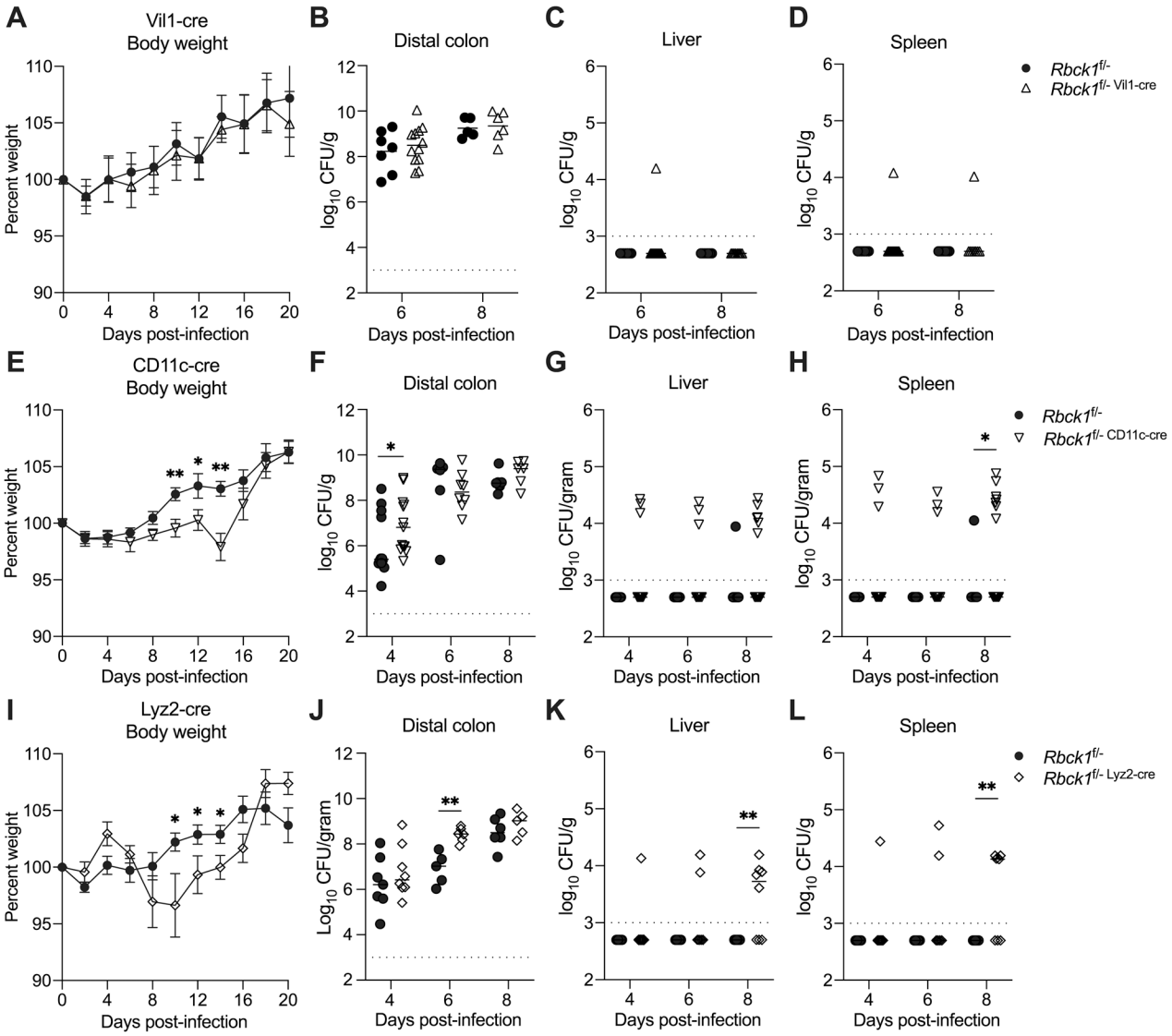


**Figure 4: HOIL1 functions in CD11c- and lysozyme 2-expressing cells to limit weight loss and systemic dissemination following *C. rodentium* infection.**

**A**. Percent body weight of *Rbck1*$^{f/-}$ (circles, $n = 5$) and *Rbck1*$^{f/-\ Vil1\text{-}cre}$ (triangles, $n = 6$) mice at the indicated times following i.g. inoculation with *C. rodentium*. **B-D**. *C. rodentium* CFU in distal colon (B), liver (C) and spleen (D) from *Rbck1*$^{f/-}$ and *Rbck1*$^{f/-\ Vil1\text{-}cre}$ mice at 6 and 8 dpi. **E**. Percent body weight of *Rbck1*$^{f/-}$ (circles, $n = 8$) and *Rbck1*$^{f/-\ CD11c\text{-}cre}$ (inverted triangles, $n = 11$) mice at the indicated times following i.g. inoculation. **F-H**. *C. rodentium* CFU in distal colon (F), liver (G) and spleen (H) from *Rbck1*$^{f/-}$ and *Rbck1*$^{f/-\ CD11c\text{-}cre}$ mice at 4, 6, and 8 dpi. **I**. Percent body weight of *Rbck1*$^{f/-}$ (circles, $n = 11$) and *Rbck1*$^{f/-\ Lyz2\text{-}cre}$ (diamonds, $n = 10$) mice at the indicated times following i.g. inoculation. **J-L**. *C. rodentium* CFU in distal colon (J), liver (K) and spleen (L) from *Rbck1*$^{f/-}$ and *Rbck1*$^{f/-\ Lyz2\text{-}cre}$ mice at 4, 6, and 8 dpi. For A, E and I, data represent the mean ± SEM. For all other panels, each symbol represents an individual mouse, and bars indicate the median. Dotted lines indicate the LOD. Data were combined from at least three independent experiments. Statistical analyses performed by *t*-test with Welch correction (A,

E, I) or Mann-Whitney test (B-D, F-H, J-L). *$p \leq 0.05$, **$p \leq 0.01$. See Supplementary Table I for $n$ values for tissue CFU.

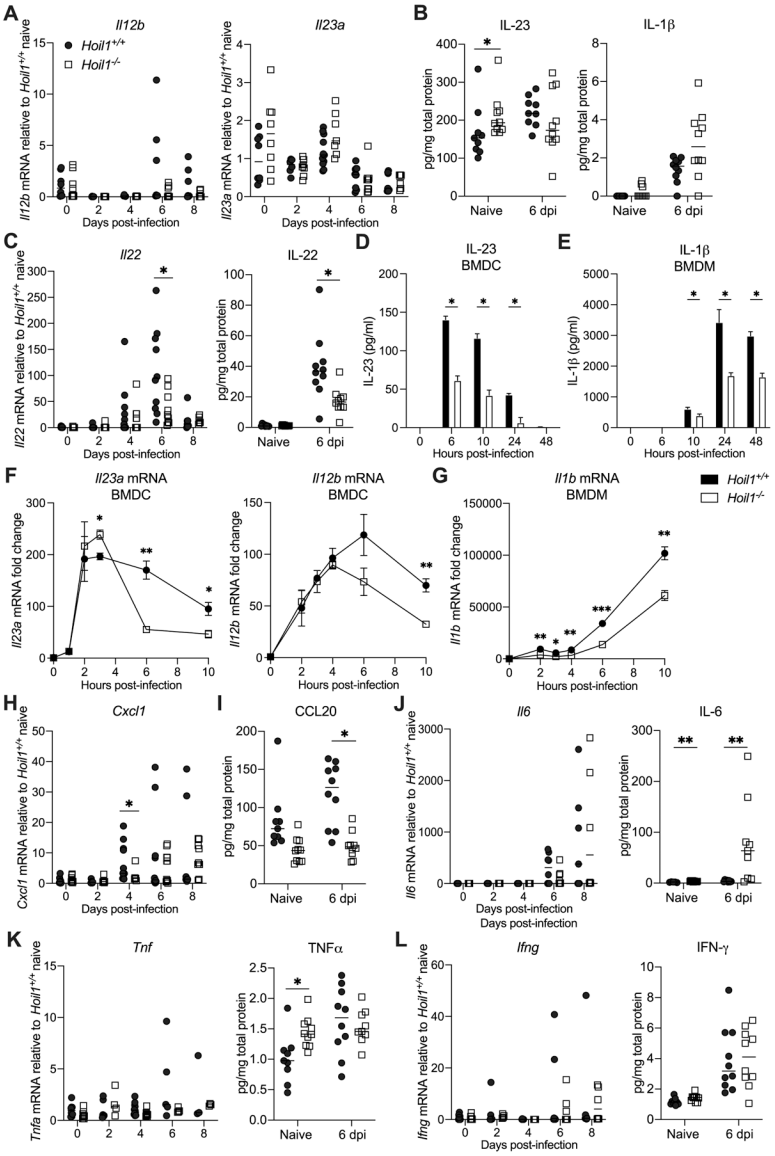


**Figure 5: HOIL1 modulates the induction of a subset of cytokines in the colon during *C. rodentium* infection.**

**A-C and H-L.** Relative cytokine mRNA levels in the distal colon over 8 d in *Hoil1*$^{+/+}$ (circles) and *Hoil1*$^{-/-}$ (squares) mice following i.g. infection with 2×10$^{9}$ CFU *C. rodentium*, and protein concentrations in homogenized colon from naïve mice and at 6 dpi. **A**. *Il12b* mRNA (left), *Il23a* mRNA (right). **B**. IL-23 protein (left), IL-1β protein (right). **C**. *Il22* mRNA (left) and IL-22 protein (right). **D**-**E**. IL-23 (D) and IL-1β (E) in cell supernatants at the indicated times post-infection. **F**-**G**. *Il23a*, *Il12b* (F) and *Il1b* mRNA (G) mRNA induction in the indicated cell types over 10 hpi. Data represent the mean ± SEM. **H**. *Cxcl1* mRNA. **I.** CCL20 protein. **J**. *Il6* mRNA (left) and IL-6 protein (right). **K**. *Tnf* mRNA (left) and TNF-α protein (right). **L**. *Ifng* mRNA (left) and IFN-γ protein (right). Each symbol represents an individual mouse, and bars indicate the median. mRNA values are relative to *Hoil1*$^{+/+}$ uninfected. Data were combined from at least three independent experiments.

Statistical analyses performed by Mann-Whitney test (A-C, H-L) or *t*-test (D-G). *$p \leq 0.05$, **$p \leq 0.01$, ***$p \leq 0.001$.

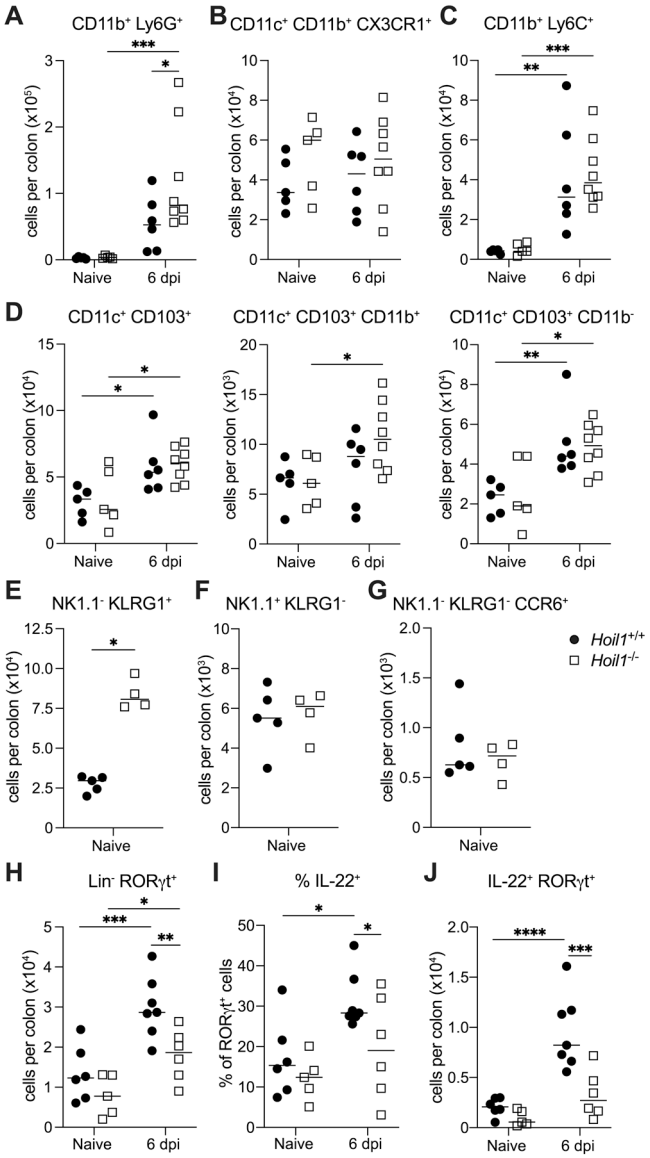


**Figure 6: HOIL1 regulates ILC3 numbers and IL-22 expression in the colon.**

Quantification of innate immune cell populations in the colonic lamina propria from naïve *Hoil1*$^{+/+}$ (filled circles) and *Hoil1*$^{-/-}$ (open squares) mice and at 6 dpi with *C. rodentium*. Pre-gated on live, CD45$^+$ singlets. **A**. CD11b$^+$ Ly6G$^+$ (neutrophils). **B**. CD11c$^+$ CD11b$^+$ CX3CR1$^+$ (resident macrophages). **C**. CD11b$^+$ Ly6C$^+$ (inflammatory monocytes). **D**. CD11c$^+$ CD103$^+$ (left), CD11c$^+$ CD103$^+$ CD11b$^+$ (middle), and CD11c$^+$ CD103$^+$ CD11b$^-$ (right) (dendritic cells). **E**. Lin$^-$ CD90.2$^+$ NK1.1$^-$ KLRG1$^+$ (ILC2). **F**. Lin$^-$ CD90.2$^+$ NK1.1$^+$ KLRG1$^-$ (ILC1). **G**. Lin$^-$ CD90.2$^+$ KLRG1$^-$ NK1.1$^-$ CCR6$^+$ (CCR6$^+$ ILC3). **H**. Lin$^-$ CD90.2$^+$ KLRG1$^-$ NK1.1$^-$ RORγt$^+$ (ILC3). **I**. Percentage of RORγt$^+$ ILC3 (from H) expressing IL-22. **J**. Lin$^-$ CD90.2$^+$ KLRG1$^-$ NK1.1$^-$ RORγt$^+$ IL-22$^+$ (IL-22$^+$ ILC3). Lineage markers: CD3, CD5, B220, CD19, TCRβ, TCRγδ. Each symbol represents an individual mouse and bars indicate the median. Data combined from at least three independent experiments. Statistical analyses performed by two-way ANOVA with

Tukey's multiple comparisons test (A-D, H-J) or Mann-Whitney (E-G). *$p \leq 0.05$, **$p \leq 0.01$, ***$p \leq 0.001$, ****$p \leq 0.0001$. See Supplementary Fig. 2 for gating strategies.